Cell Reports
Medicine

Article

Microglial CMPK2 promotes neuroinflammation and brain injury after ischemic stroke

Graphical abstract

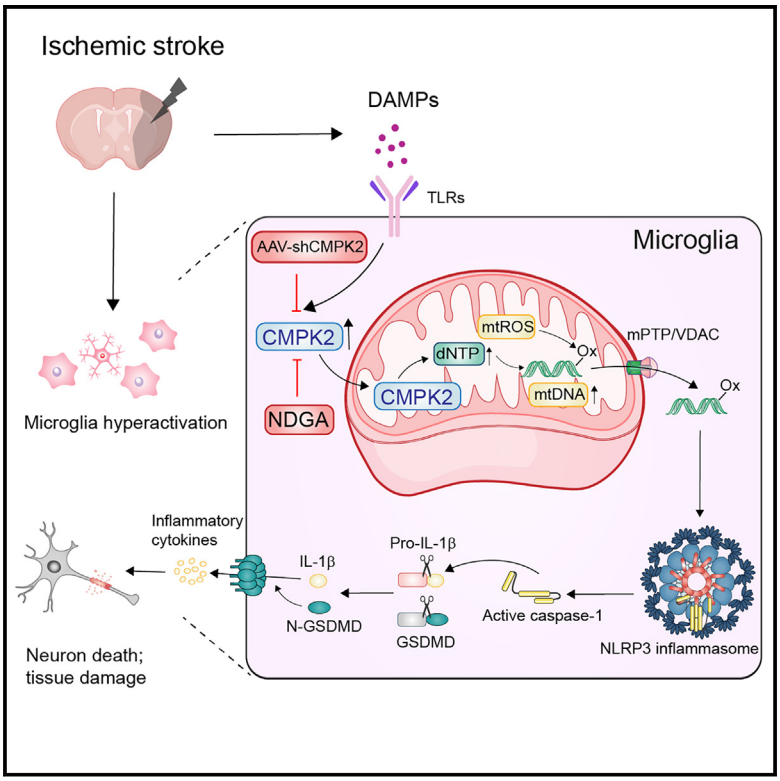

Highlights

- CMPK2 expression is increased in microglia/macrophages after ischemic stroke
- CMPK2 knockdown in microglia/macrophages ameliorates ischemic injury in mice
- CMPK2 inhibitor nordihydroguaiaretic acid ameliorates ischemic injury in mice

Authors

Xin Guan, Sitong Zhu, Jinqian Song, ..., Jin Wu, Xiaojun Xu, Tao Pang

Correspondence

wujin@njmu.edu.cn (J.W.), xiaojunxu@zju.edu.cn (X.X.), tpang@cpu.edu.cn (T.P.)

In brief

Neuroinflammation promotes brain ischemic injury. Guan et al. show that mitochondrial CMPK2 is induced after ischemic insults in monocytes/macrophages and microglia and participates in neuroinflammation. AAV-mediated CMPK2 knockdown in microglia/macrophages, or the CMPK2 inhibitor nordihydroguaiaretic acid, reduces neuroinflammation and ameliorates ischemic injury, indicating a potential therapeutic target for ischemic stroke.

Guan et al., 2024, Cell Reports Medicine 5, 101522
May 21, 2024
https://doi.org/10.1016/j.xcrm.2024.101522

CellPress

Cell Reports Medicine

CellPress
OPEN ACCESS

Article

Microglial CMPK2 promotes neuroinflammation and brain injury after ischemic stroke

Xin Guan,[1,5] Sitong Zhu,[1,5] Jinqian Song,[1] Kui Liu,[1] Mei Liu,[2] Luyang Xie,[1] Yifang Wang,[2] Jin Wu,[2,*] Xiaojun Xu,[3,*] and Tao Pang[1,4,6,*]

[1]State Key Laboratory of Natural Medicines, New Drug Screening Center, Key Laboratory of Drug Quality Control and Pharmacovigilance (Ministry of Education), China Pharmaceutical University, Nanjing 210009, P.R. China

[2]Department of Neurology, The Second Affiliated Hospital of Nanjing Medical University, Nanjing 210011, P.R. China

[3]Department of Pharmacy, The Fourth Affiliated Hospital, Zhejiang University School of Medicine, Center for Innovative Traditional Chinese Medicine Target and New Drug Research, International Institutes of Medicine, Zhejiang University, Yiwu, Zhejiang Province 322000, P.R. China

[4]State Key Laboratory of Pharmaceutical Biotechnology, Nanjing University, Nanjing 210023, P.R. China

[5]These authors contributed equally

[6]Lead contact

*Correspondence: wujin@njmu.edu.cn (J.W.), xiaojunxu@zju.edu.cn (X.X.), tpang@cpu.edu.cn (T.P.)

https://doi.org/10.1016/j.xcrm.2024.101522

SUMMARY

Neuroinflammation plays a significant role in ischemic injury, which can be promoted by oxidized mitochondrial DNA (Ox-mtDNA). Cytidine/uridine monophosphate kinase 2 (CMPK2) regulates mtDNA replication, but its role in neuroinflammation and ischemic injury remains unknown. Here, we report that CMPK2 expression is upregulated in monocytes/macrophages and microglia post-stroke in humans and mice, respectively. Microglia/macrophage CMPK2 knockdown using the *Cre* recombination-dependent adeno-associated virus suppresses the inflammatory responses in the brain, reduces infarcts, and improves neurological outcomes in ischemic $CX_3CR1^{Cre/ERT2}$ mice. Mechanistically, CMPK2 knockdown limits newly synthesized mtDNA and Ox-mtDNA formation and subsequently blocks NLRP3 inflammasome activation in microglia/macrophages. Nordihydroguaiaretic acid (NDGA), as a CMPK2 inhibitor, is discovered to reduce neuroinflammation and ischemic injury in mice and prevent the inflammatory responses in primary human monocytes from ischemic patients. Thus, these findings identify CMPK2 as a promising therapeutic target for ischemic stroke and other brain disorders associated with neuroinflammation.

INTRODUCTION

Acute ischemic stroke is a devastating acute cerebrovascular disorder,[1,2] manifesting as fast-onset muscle weakness, mental confusion, loss of balance or coordination, sudden syncope, paralysis, and other severe symptoms.[3] Despite the advancements in medical technology and surgical instruments, stroke remains the second leading cause of death globally, accounting for 11.6% of all disease mortality,[4] and ranks as the third leading cause of disability-adjusted life years (DALYs), accounting for approximately 5.7% of all DALYs.[4] Currently, intravenous thrombolysis with recombinant tissue plasminogen activator (r-tPA) is the only treatment strategy recognized as effective by all regulatory agencies.[5] Nevertheless, intravenous thrombolysis with r-tPA has strict time window limitations of approximate 4.5 h as well as medical restrictions,[6] so less than 3% of ischemic patients could benefit from it. Although numerous neuroprotective agents have displayed significant efficacy in animal experiments for decades, they have failed in clinical trials.[7] Consequently, there is an urgent need to identify potential therapeutic targets and interventions for ischemic stroke.

Multiple pathophysiological mechanisms participate in the progression of cerebral ischemic stroke, including neuroinflammatory response, calcium overload, oxidative stress, and excitotoxicity.[6] Neuroinflammation mediated by microglia exhibits crucial influences over ischemic injury and is highly correlated with long-term cognitive and motor function after stroke.[8] Upon ischemia attack, neuronal death triggers secondary immune responses characterized by microglia hyperactivation and release of cytokines and chemokines.[9] Afterward, activated microglia accumulate around the lesioned area and peri-infarct border zone, lasting from a few hours to several weeks.[8,9] In microglial mitochondria, the reactive oxygen species (ROSs) are extensively produced after stroke.[10,11] As mitochondrial DNA (mtDNA) possesses limited repair capacity and is lacking the protection of histone proteins,[12,13] mtDNA is vulnerable and easily oxidized, primarily in the form of 8-hydroxy-2-deoxyguanosine (8-OHdG).[14] The level of 8-OHdG has been validated to be highly correlated with the severity of ischemic stroke and to be an independent prognostic factor of the functional outcomes in patients with stroke.[15–19] However, it is unclear whether inhibition of oxidized

mtDNA (Ox-mtDNA) production could be an effective way to treat ischemic stroke.

Cytidine/uridine monophosphate kinase 2 (CMPK2) is a rate-limiting enzyme for the synthesis of deoxynucleoside triphosphates to regulate mtDNA replication.[14] Several reports have shown that CMPK2 participates in the progression of diseases, including acute respiratory distress syndrome (ARDS), brain calcification, spinal cord injury, and coronaviruses (CoVs).[14,20–24] mtDNA is an intramitochondrial closed double-stranded DNA circle that functions as a damage-associated molecular marker to induce inflammation.[14,25] Under normal physiological circumstances, on the one hand, transcription factor A (TFAM) can promote the packaging and compaction of naked mtDNA into nucleoids,[14] thereby minimizing susceptibility to mitochondrial ROS (mtROS); on the other hand, timely termination of inflammation evoked by mtDNA can promote tissue repair and help re-establish homeostasis in the host by clearing pathogens.[14] However, under pathological states, ROSs, pathogen-associated molecular patterns, and damage-associated molecular patterns (DAMPs) can prompt mitochondrial permeability transition pore (mPTP) opening and voltage-dependent anion channel (VDAC) oligomerization in mitochondrial membranes to facilitate mtDNA release to the cytoplasm.[14,25,26] mtROS does not directly induce inflammasome activation,[26] but mtDNA oxidized by mtROS (Ox-mtDNA) can directly activate the NLRP3 inflammasome to induce cleaved caspase-1 and mature interleukin (IL)-1β secretion. The upregulation of CMPK2 expression could initiate new synthesis of naked and uncompacted mtDNA in lipopolysaccharide (LPS)-primed immune cells to trigger inflammasome-mediated inflammation.[14,25,26] Despite considerable studies highlighting the pivotal roles of CMPK2 in diseases including ARDS, brain calcification, spinal cord injury, and CoVs,[14,20–24] little is yet known about the role of CMPK2 in cerebral ischemic stroke.

In this study, we investigated the function of CMPK2 in ischemic stroke. We found that adeno-associated virus (AAV)-mediated microglia/macrophage CMPK2 knockdown in $CX_3CR1^{Cre/ERT2}$ mice, or a natural product, nordihydroguaiaretic acid (NDGA), identified as a specific CMPK2 inhibitor, reduced brain injury and presented better long-term neurological outcomes after transient middle cerebral artery occlusion (tMCAO) treatment. Moreover, microglia/macrophage CMPK2 knockdown or NDGA treatment inhibited the expression of newly synthesized mtDNA and Ox-mtDNA formation and subsequently limited NLRP3 inflammasome activation. Our study laid the foundation for CMPK2 as a potential therapeutic target for ischemic stroke and other neurological disorders associated with neuroinflammation.

RESULTS

Peripheral blood expression of CMPK2 is upregulated in patients with stroke and correlated with infarct volume

Gene expression variability in peripheral whole blood between healthy subjects and patients with ischemic stroke, which has been recognized as an approach to identify valuable biomarkers or predictors for the diagnosis or prognosis of ischemic stroke,[27,28] has garnered investigators' interest for decades. Currently, the precise role of CMPK2 in the pathological processes of ischemic stroke remains to be elucidated. We evaluated *CMPK2* gene expression in peripheral whole blood and discovered that *CMPK2* gene expression was highly elevated in patients with ischemic stroke compared with that in the control subjects (Figure 1A). We subsequently analyzed the relationship between *CMPK* gene expression and infarct volume or National Institutes of Health Stroke Scale (NIHSS) score. We observed a positive correlation between *CMPK2* gene expression and infarct volume or NIHSS score, indicating that CMPK2 may be positively correlated with stroke severity in patients (Figures 1B–1D). Afterward, we evaluated the changes of mtDNA levels in the peripheral blood of patients with stroke by examining the expressions of representative mtDNA markers, including displacement loop (*D-LOOP*), *COX1*, *CYTB*, and nDNA (*TERT*).[29,30] The results revealed that the expressions of *D-LOOP*, *COX-1*, and *CYTB* were upregulated in patients with stroke in comparison to control subjects (Figure S1A). Then, we examined the expression of 8-OHdG, the biomarker of Ox-mtDNA, which is promoted by CMPK2 upregulation.[14] Immunofluorescence analyses showed that 8-OHdG expression and CMPK2 expression were increased in peripheral whole blood after stroke onset relative to that of the control subject (Figures 1E–1H). Moreover, we observed that 8-OHdG expression was obviously increased in $CD11b^+$ cells (Figures S1B and S1C). These findings demonstrated that elevated CMPK2 levels in peripheral whole blood correlated positively with stroke severity in human stroke subjects.

CMPK2 is a microglia/macrophage-specific regulator after ischemic stroke onset

Coincident with the finding in human peripheral blood, we discovered that CMPK2 protein expression was significantly elevated at 3 h, peaked at 24 h, and finally returned to baseline at 7 days in the brain peri-infarct region in the mouse or rat tMCAO model (Figures 2A, 2B, S2A, and S2B). Subsequently, we investigated which cell type would increase CMPK2 expression in the ischemic hemisphere. Immunofluorescence staining results revealed that CMPK2 expression was obviously increased in microglia/macrophages, but not astrocytes or neurons, after stroke onset (Figures 2C, 2D, S2C, and S2D). To further determine the expression of CMPK2 in microglia/macrophages after ischemia attack, we isolated microglia/macrophages by magnetic bead sorting (Figures S2E and S2F). Also, we observed a significant increase in CMPK2 expression in microglia/macrophages at 24 h post-stroke compared with the sham group (Figures 2E and 2F).

Then, to simulate the *in vivo* cerebral ischemia, the oxygen-glucose deprivation (OGD)-induced cell death model was established in primary mouse astrocytes, microglia, and cortical neurons *in vitro*. Consistent with the findings of *in vivo* experiments, CMPK2 expression was markedly elevated in a time-dependent manner and peaked at 6 h in primary mouse microglia (Figures 2G and 2H). However, after OGD conditions, primary neurons displayed slight upregulation in CMPK2 expression, and primary astrocytes displayed no discernible change in CMPK2 expression (Figures 2I, 2J, and S2G–S2J). Overall, these data demonstrated that CMPK2 expression was predominantly

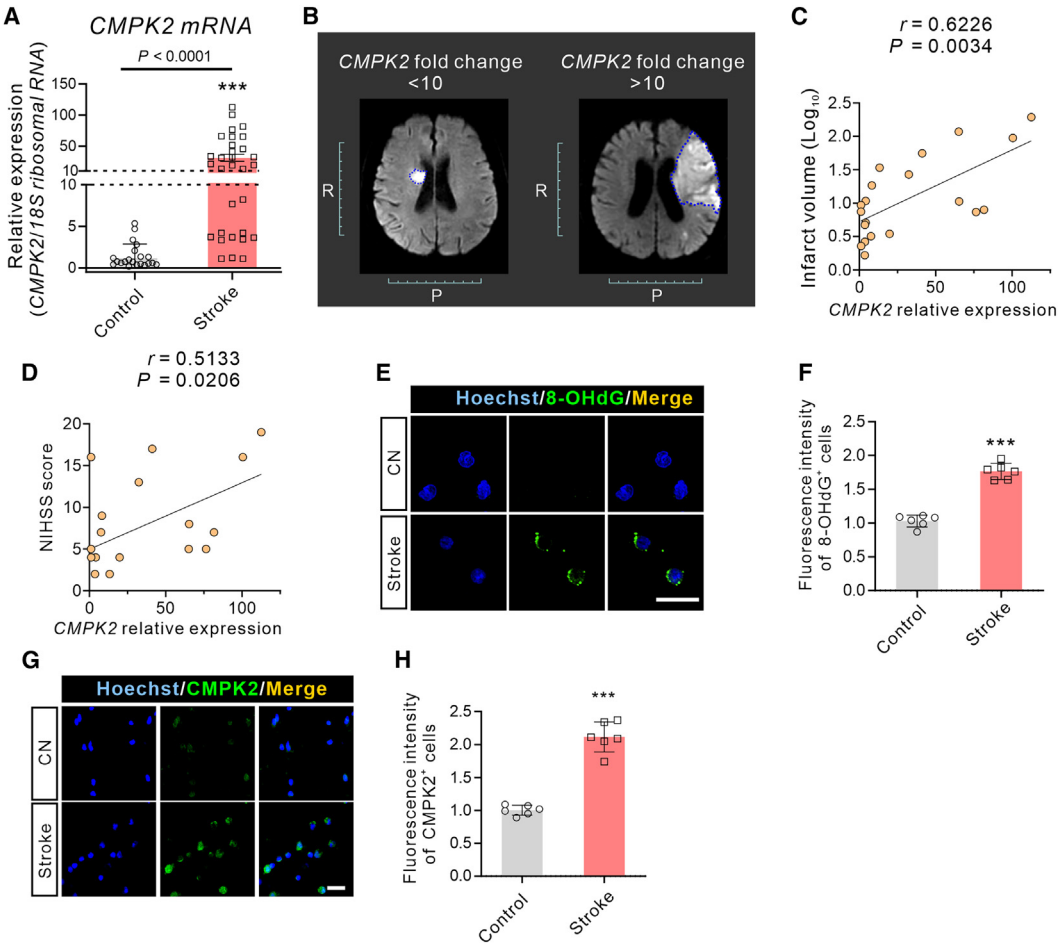

Figure 1. Peripheral blood expression of CMPK2 is elevated and positively correlative with infarct volume in human ischemic subjects

(A) Quantification for *CMPK2* gene expression (control = 21, stroke = 31).

(B) Representative magnetic resonance imaging (MRI) images (diffusion-weighted imaging) of patients with stroke with *CMPK2* gene expression (fold change < 10 and fold change > 10).

(C) The correlation analysis was performed between *CMPK2* transcript levels in blood and infarct volume in patients with stroke. $n = 20$.

(D) The correlation analysis was performed between *CMPK2* transcript levels in blood and NIHSS score in patients with stroke. $n = 20$.

(E and F) Representative immunofluorescence images and quantification of 8-OHdG expression levels in the peripheral blood of ischemic patients. Scale bar: 20 μm. $n = 6$.

(G and H) Representative immunofluorescence images and quantification of CMPK2 expression levels in the peripheral blood of patients with acute ischemic stroke. Scale bar: 20 μm. $n = 6$.

Results are represented as means ± SD. ***$p < 0.001$ vs. non-stroke control subjects.

increased in microglia/macrophages in the ischemic brain during the acute phase of stroke.

Microglia/macrophage CMPK2 knockdown protects against ischemic brain injury in the mouse tMCAO model

According to the previous literature,[31] $CX_3CR1^{Cre/ERT2}$ mice were microinjected with microglia/macrophage-specific adeno-associated virus (AAV)-CMPK2 short hairpin RNA (AAV-U6-LoxP-CMV-mCherry-LoxP-CMPK2-shRNA-WPRE-poly(A) [AAV-shCMPK2]) or the scrambled control AAV (AAV-U6-LoxP-CMV-mCherry-LoxP-scramble-shRNA-WPRE-poly(A) [AAV-shCon]) in the right cortex, followed by administration with tamoxifen for 5 consecutive days (Figure 3A). We examined the transfection efficiency of mCherry-tagged AAV and observed that mCherry was primarily detected in microglia/macrophages, with little colocalization with neurons or astrocytes (Figures 3B and S3A–S3C). The immunohistochemical staining and western blotting results showed that CMPK2 expression was obviously downregulated in microglia/macrophages in the cerebral cortex of AAV-shCMPK2 $CX_3CR1^{Cre/ERT2}$ mice (Figures 3C, 3D, and S3D–S3G). Next, we explored whether microglial proliferation after stroke onset affected CMPK2 knockdown efficiency by western blotting. We isolated primary mouse microglia cells from $CX_3CR1^{Cre/ERT2}$ mice at postnatal days 1–3 and then supplemented them with mouse recombinant macrophage colony-stimulating factor (MCSF) protein for 48 h to stimulate the microglial proliferation according to previous literature.[32] The western blotting analysis

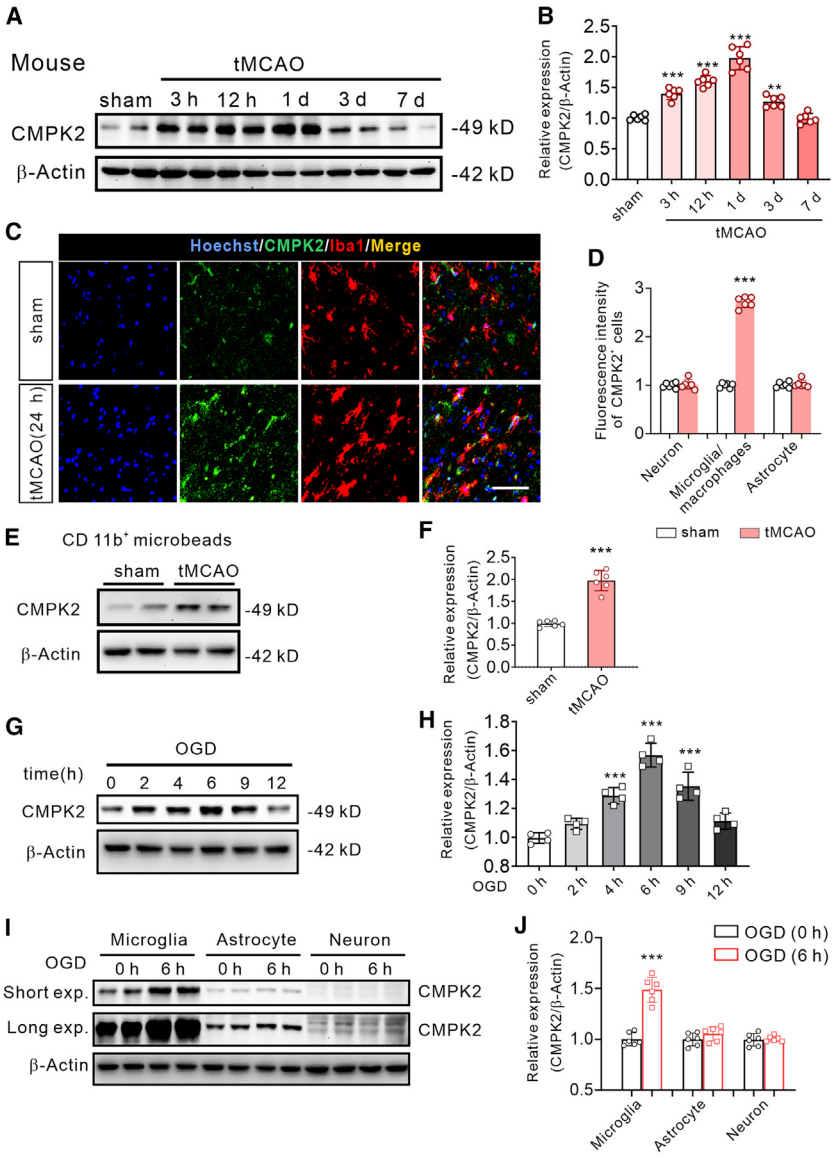

Figure 2. CMPK2 expression is mainly upregulated in microglia/macrophages of the brain after ischemia onset

(A and B) Western blotting images and quantification for CMPK2 protein expression in the peri-infarct region of sham-operated and ischemic mice at 3 h, 12 h, 1 day, 3 days, and 7 days following operation. $n = 6$.

(C and D) Representative immunofluorescence images and quantitative analysis of $CMPK2^{+}$ $Iba1^{+}$ cells in the peri-infarct region of the ischemic mice. Scale bar: 50 μm. $n = 6$.

(E and F) Western blotting images and quantification for CMPK2 protein expression in microglia/macrophages isolated from the peri-infarct region with $CD11b^{+}$ magnetic beads at 24 h following operation. $n = 6$.

(G and H) Western blotting images and quantification for CMPK2 expression in primary mouse microglia exposed to OGD conditions for 0, 2, 4, 6, 9, or 12 h. $n = 4$.

(I and J) Western blotting images and quantification for CMPK2 expression in primary mouse microglia, astrocytes, or cortical neurons exposed to OGD conditions for 0 and 6 h. $n = 6$.

Results are represented as means ± SD. $^{**}p < 0.01$ and $^{***}p < 0.001$ vs. sham or 0 h group.

indicated that transfection with AAV-shCMPK2 small interfering RNAs (siRNAs) could effectively reduce the protein expression of CMPK2 to approximately 50% compared to cells transfected with AAV-shCon subjected to MCSF stimulation (Figure S3H). Thus, supported by the above findings, we validated that CMPK2 shRNA-specific targeting to microglia/macrophages was established in $CX_3CR1^{Cre/ERT2}$ mice. Subsequently, we developed the mouse tMCAO model to seek out the potential effects of microglial CMPK2 on cerebral ischemic damage. We initially assessed the regional cerebral blood flow (rCBF) to exclude the possibilities of variations in cerebral vessel congestion and eventually verified that there existed no apparent differences in the rCBF at baseline, during ischemia, or after reperfusion between the AAV-shCon and AAV-shCMPK2 $CX_3CR1^{Cre/ERT2}$ mice (Figures 3E and 3F). Then, after ischemia attack, AAV-shCMPK2 $CX_3CR1^{Cre/ERT2}$ mice displayed markedly ameliorated ischemic volume as determined by 2,3,5-triphenyltetrazolium chloride (TTC) staining and significantly improved short-term neurological outcomes as indicated by lower scores in the Longa test in comparison to the AAV-shCon $CX_3CR1^{Cre/ERT2}$ mice (Figures 3G and 3H). Moreover, we also found that less ischemic volume and improved neurological functions existed in the AAV-shCMPK2 $CX_3CR1^{Cre/ERT2}$ female mice compared with AAV-shCon $CX_3CR1^{Cre/ERT2}$ female mice following ischemic stroke (Figures 3I and 3J). Based on the aforementioned finding, we conclude that microglia/macrophage-specific CMPK2 knockdown ameliorates ischemic injury in the mouse tMCAO model.

Microglia/macrophage CMPK2 knockdown improves the long-term functional performances in the mouse tMCAO model

The prognosis and quality of life of long-term stroke survivors are correlated with motor function recovery post-ischemic stroke.[33] To further investigate the effects of CMPK2 on long-term functional outcomes after ischemia onset, we conducted longitudinal T2-weighted MRI scanning and a series of long-term functional tests on the AAV-shCon and AAV-shCMPK2 $CX_3CR1^{Cre/ERT2}$ mice subjected to ischemic stroke (Figure 4A). MRI scanning revealed obviously enlarged ischemic lesions in the AAV-shCon $CX_3CR1^{Cre/ERT2}$ mice at 14 days after tMCAO, whereas the AAV-shCMPK2 injection in the $CX_3CR1^{Cre/ERT2}$ mice efficiently

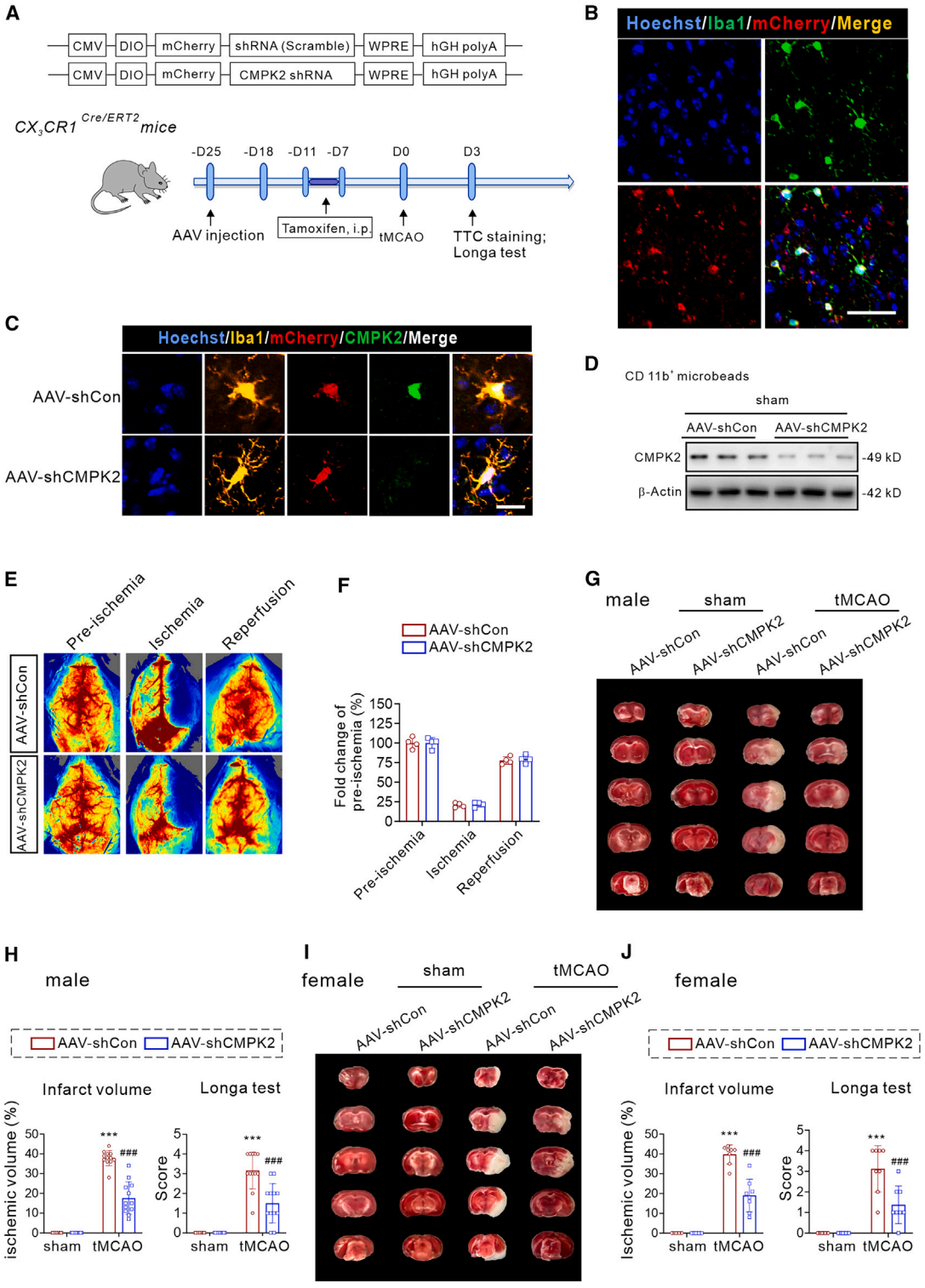

Figure 3. Microglia/macrophage CMPK2 silencing reduces brain ischemic volume and improves short-term neurological function in the mouse tMCAO model

(A) Schematic diagram about experimental strategy for CMPK2 knockdown.

(B) Representative immunofluorescence images of mCherry$^+$ cells stained with Iba1. Scale bar: 50 μm. $n = 4$.

(C) Representative immunofluorescence images of mCherry$^+$ cells stained with Iba1 and CMPK2. Scale bar: 20 μm. $n = 6$.

(legend continued on next page)

reduced the infarct volume (Figures 4B and 4C). In addition, AAV-shCMPK2 treatment significantly ameliorated long-term functional deficits in the $CX_3CR1^{Cre/ERT2}$ mice, as revealed by the markedly reduced score in the modified neurological severity score (mNSS) test, enhanced score in the wire-hanging test, decreased percentage of forelimb faults in foot missteps, and increased time in the rotarod test in contrast to the AAV-shCon $CX_3CR1^{Cre/ERT2}$ mice 0, 3, 5, 7, 14, 21, and 28 days post-ischemia (Figure 4D). Furthermore, AAV-shCMPK2 administration substantially enhanced the survival proportions during the relatively delayed stage (28 days) compared to ischemic AAV-shCon $CX_3CR1^{Cre/ERT2}$ mice (Figure 4E). These results highlighted that CMPK2 in microglia/macrophages contributed, at least partly, to ischemic injury and poor long-term functional performances after ischemic stroke.

Microglia/macrophage CMPK2 knockdown promotes microglial ramification and inhibits Ox-mtDNA-induced NLRP3 inflammasome activation in the brain of ischemic mice

Microglia morphology is highly plastic and rapidly changes to closely monitor and regulate neuronal functions in response to varying environmental situations, especially ischemic insult.[34,35] To seek out the potential mechanism underlying microglial protection against ischemic stroke, we assessed the influences of microglia/macrophage CMPK2 silencing on microglial morphology. We observed that microglial morphology was more ramified and homeostatic-like in the AAV-shCMPK2 $CX_3CR1^{Cre/ERT2}$ mice than in the AAV-shCon $CX_3CR1^{Cre/ERT2}$ mice at 3 days after ischemia (Figure 5A). Particularly, the morphometric analysis indicated that the AAV-shCMPK2 treatment could increase the process lengths and the number of branches compared to the AAV-shCon treatment (Figure 5B). In addition, ramified microglial cells were accompanied by less proliferation ability.[36] Then, to evaluate whether CMPK2 knockdown influences microglia proliferation in the mouse tMCAO model *in vivo*, we conducted immunofluorescence staining by costaining Ki67 with Iba1, according to previous reports,[37,38] and found that no statistical differences were observed in the numbers of $Ki67^+$ $Iba1^+$ cells between the AAV-shCon and AAV-shCMPK2 $CX_3CR1^{Cre/ERT2}$ mice (Figure S4A). To evaluate the effects of CMPK2 knockdown on microglia proliferation *in vitro*, we established an MCSF-induced proliferation model in mouse primary microglia cells and applied EdU staining according to previous literature.[38] The immunofluorescence results of EdU staining indicated that the MCSF-induced microglia proliferation was not influenced by CMPK2 knockdown (Figure S4B). Thus, CMPK2 knockdown did not affect microglia proliferation *in vivo* and *in vitro*. Consequently, these data demonstrated that CMPK2 knockdown inhibited microglial hyperactivation following ischemic insult.

We then explored the effects of microglia/macrophage CMPK2 silencing on 8-OHdG, which is the biomarker of Ox-mtDNA. As illustrated by Figures 5C–5F, the immunofluorescence analysis results demonstrated that the 8-OHdG level was significantly elevated in microglia in the AAV-shCon $CX_3CR1^{Cre/ERT2}$ mice, but substantially decreased in the peri-infarct area of AAV-shCMPK2 $CX_3CR1^{Cre/ERT2}$ mice, at 24 and 72 h after ischemia.

Ox-mtDNA mediated by CMPK2 could drive NLRP3 inflammasome activation,[26] which eventually promotes uncontrolled inflammation and death in the neighboring cell.[39,40] Compared to sham-operated $CX_3CR1^{Cre/ERT2}$ mice, the protein expressions of bioactive gasdermin D N-terminal fragment (N-GSDMD [p30]), cleaved caspase-1 (caspase-1 p20), and mature IL-1β (IL-1β p17) were obviously upregulated in the peri-infarct region after AAV-shCon administration, which was significantly reduced after AAV-shCMPK2 treatment in the peri-infarct region of $CX_3CR1^{Cre/ERT2}$ mice at 3 days after ischemia (Figure 5G). Based on the aforementioned findings, we conclude that CMPK2 could promote mtDNA replication to stimulate Ox-mtDNA formation and subsequently trigger NLRP3 inflammasome activation in microglia/macrophages after ischemic stroke.

CMPK2 facilitates Ox-mtDNA formation and NLRP3 inflammasome activation in primary mouse microglia cells

To validate these findings from *in vivo* experiments, we investigated the effects of CMPK2 on Ox-mtDNA formation in primary mouse microglia cells *in vitro*. Priming with LPSs followed by ATP stimulation is a well-established model to activate the NLRP3 inflammasome in primary mouse microglia cells[41–43] and has been implicated in a plethora of literature exploring the pathological mechanisms of microglia in the context of ischemic stroke.[34,43] First, we examined the gene and protein expressions of CMPK2 in microglia stimulated with LPS. As depicted in the Figures S5A–S5C, the gene and protein expressions of CMPK2 were significantly increased from 3 to 12 h after LPS stimulation. Afterward, we confirmed that CMPK2 siRNA potently reduced CMPK2 protein expression in primary mouse microglia cells relative to the control group, with or without LPS stimulation (Figures S5D–S5G). Then, we observed significant increases of cleaved caspase-1, N-GSDMD, and mature IL-1β in the cell supernatant of LPS-primed microglia cells followed by stimulation with ATP, which were significantly suppressed by CMPK2 knockdown in primary mouse microglia (Figures S5H–S5J). Lactate dehydrogenase (LDH) assay analysis showed that LPS plus ATP stimulation induced LDH release in the supernatant

(D) Western blotting images for CMPK2 protein expression in microglia/macrophages isolated from the brain of AAV-shCon and AAV-shCMPK2 $CX_3CR1^{Cre/ERT2}$ mice with $CD11b^+$ magnetic beads. $n = 6$.
(E and F) Regional cerebral blood flow. Results are expressed as means ± SD. $n = 4$.
(G and H) AAV-shCMPK2 administration reduced cerebral infarct volume and promoted neurological functions in $CX_3CR1^{Cre/ERT2}$ male mice. $n = 12$.
(I and J) AAV-shCMPK2 administration toned down cerebral infarct volume and improved neurological function in the $CX_3CR1^{Cre/ERT2}$ female mice. $n = 8$. Results are represented as means ± SD.
$^{***}p < 0.001$ vs. sham plus AAV-shCon group and $^{\#\#\#}p < 0.001$ vs. tMCAO plus AAV-shCon group.

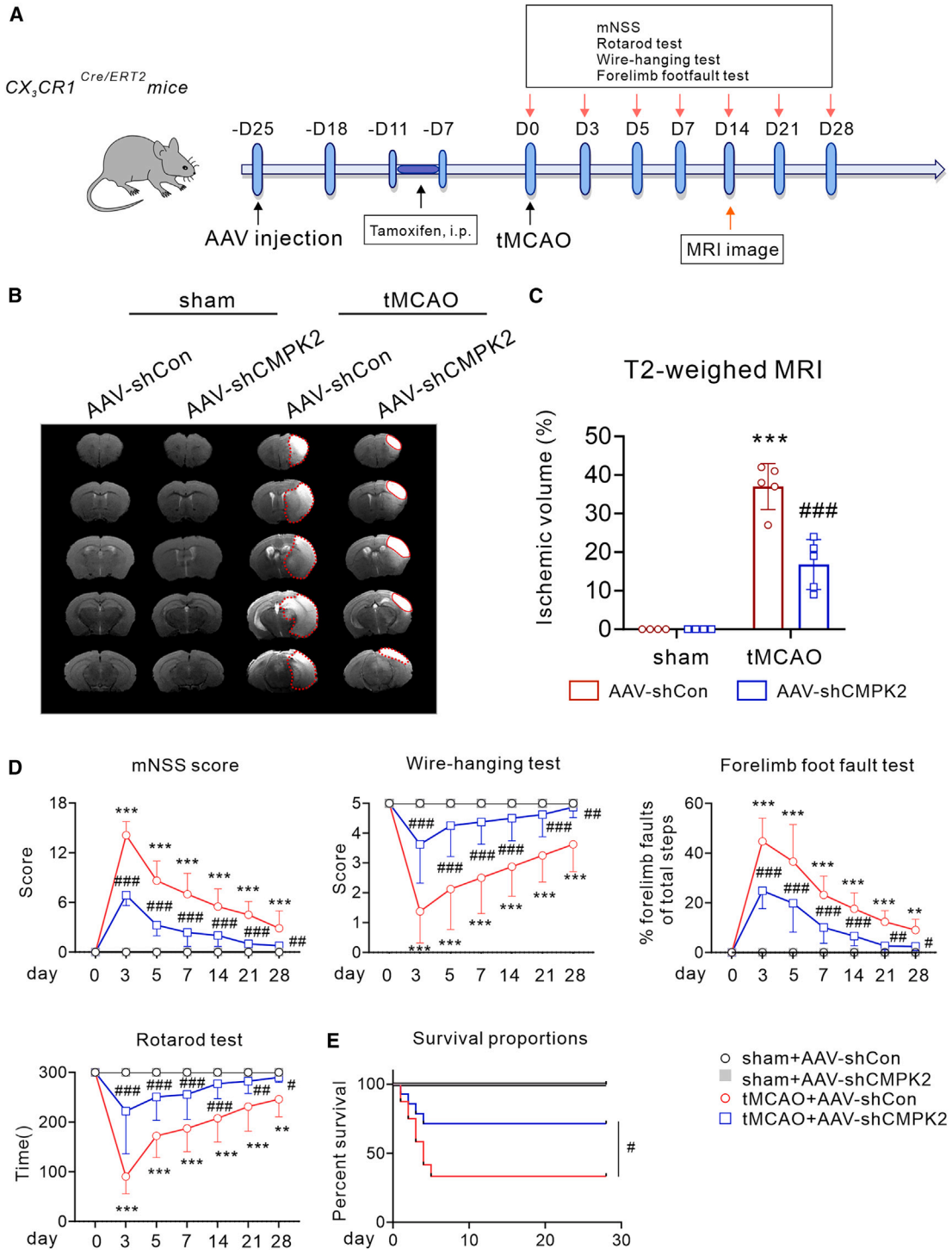

Figure 4. Microglia/macrophage CMPK2 silencing reduces brain infarction and improves long-term functional performances in the mouse tMCAO model

(A) Schematic diagram about experimental procedures.

(B and C) Representative T2-weighted MRI images of $CX_3CR1^{Cre/ERT2}$ mice on day 14 post-tMCAO. $n = 4$ or 5.

(D) The long-term functional performances were investigated in $CX_3CR1^{Cre/ERT2}$ mice. $n = 8$.

(E) The survival proportions. $n = 12–15$.

Results are represented as means ± SD. $^{**}p < 0.01$ and $^{***}p < 0.001$ vs. sham plus AAV-shCon group and $^{\#}p < 0.05$, $^{\#\#}p < 0.01$, and $^{\#\#\#}p < 0.001$ vs. tMCAO plus AAV-shCon group.

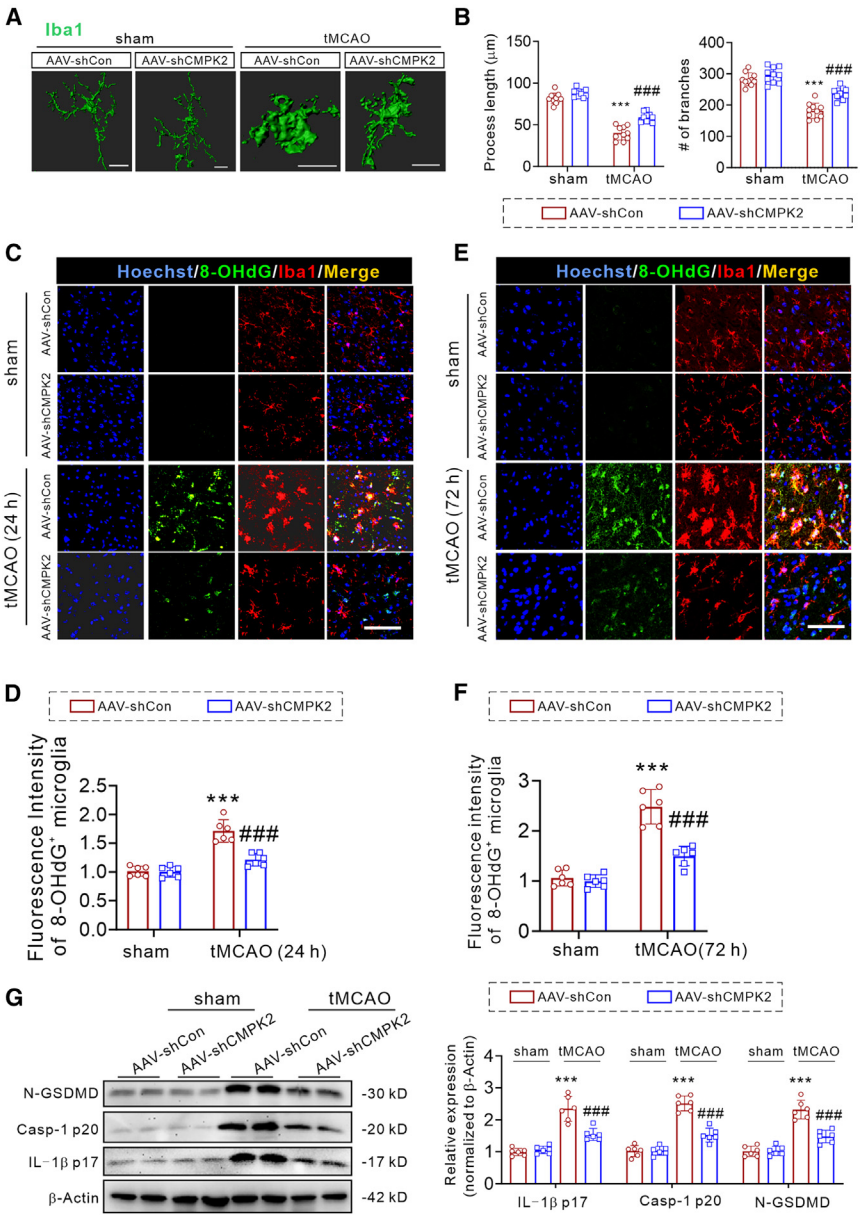

Figure 5. Microglia/macrophage CMPK2 silencing promotes microglial ramification and disrupts Ox-mtDNA-induced NLRP3 inflammasome activation in the brain of ischemic mice

(A) Imaris-based 3D reconstruction images of microglia immunofluorescently stained with Iba1. Scale bar: 15 μm.

(B) The process length and the number of branches of microglia stained with Iba1 in AAV-shCon and AAV-shCMPK2 $CX_3CR1^{Cre/ERT2}$ mice at 3 days after ischemia. $n = 10$. Results are represented as means ± SD.

(C–F) Representative immunofluorescence images and quantification of microglia/macrophages stained with 8-OHdG and quantitative analysis of 8-OHdG$^+$ Iba1$^+$ cells in the peri-infarct region of $CX_3CR1^{Cre/ERT2}$ mice at 24 and 72 h after ischemia. Scale bar: 50 μm. $n = 6$.

(G) Western blotting images and quantification for cleaved caspase-1, mature IL-1β, and N-GSDMD in the peri-infarct region of AAV-shCon and AAV-shCMPK2 $CX_3CR1^{Cre/ERT2}$ mice at 3 days following ischemic stroke. $n = 6$. Results are represented as means ± SD.

$^{***}p < 0.001$ vs. sham plus AAV-shCon group and $^{###}p < 0.001$ vs. tMCAO plus AAV-shCon group.

of primary mouse microglia cells, which was remarkably attenuated by CMPK2 knockdown, suggesting the inhibition of CMPK2 on pyroptosis (Figure S5K). To mimic cerebral ischemia conditions *in vitro*, we further applied OGD conditions and found that CMPK2 knockdown inhibited LDH release after OGD stimulation (Figure S5L). Collectively, these results indicated that CMPK2 knockdown inhibited NLRP3 inflammasome activation and pyroptosis in microglia subjected to LPS plus ATP stimulation or OGD conditions.

Furthermore, we examined the effects of CMPK2 on mtDNA synthesis and Ox-mtDNA production. CMPK2 knockdown decreased the expressions of *D-loop*, *Cox-1*, and *CYTB*, which were upregulated in primary mouse microglia cells in response to LPS (Figures S6A–S6C). In addition, CMPK2 silencing blocked the replication of newly synthesized mtDNA in microglia subjected to LPS stimulation or the OGD model (Figures S6D–S6G). Furthermore, we observed a significant increase in the 8-OHdG level following LPS plus ATP stimulation or OGD treatment, which was significantly suppressed by CMPK2 knockdown in microglia (Figures S6H–S6K).

Then, we assessed the potential effects of CMPK2 knockdown on mitochondrial functions, including bioenergetics, biogenesis, and morphology. Firstly, we evaluated mitochondrial bioenergetics by measuring intracellular ATP levels according to previous studies[32,44,45] and discovered that CMPK2 knockdown, followed by LPS plus ATP stimulation, did not influence the intracellular ATP level in primary mouse microglia cells (Figure S7A). Then, we measured the protein expression of PGC-1α and NRF1, which are widely recognized as pivotal regulators of mitochondrial biogenesis.[32,46,47] Western blotting analysis showed that the protein expressions of PGC-1α and NRF1 were significantly reduced in the microglial cells after LPS plus ATP stimulation, and they were also not influenced by CMPK2 knockdown (Figures S7B and S7C). Afterward, we assessed the changes of mitochondrial morphology outlined by TOMM20 antibodies according to previous studies.[45,48] The immunofluorescence analyses showed that, compared to the controls, the mitochondria turned out to be obviously more fragmented after LPS plus ATP stimulation, which could be mitigated by CMPK2 knockdown

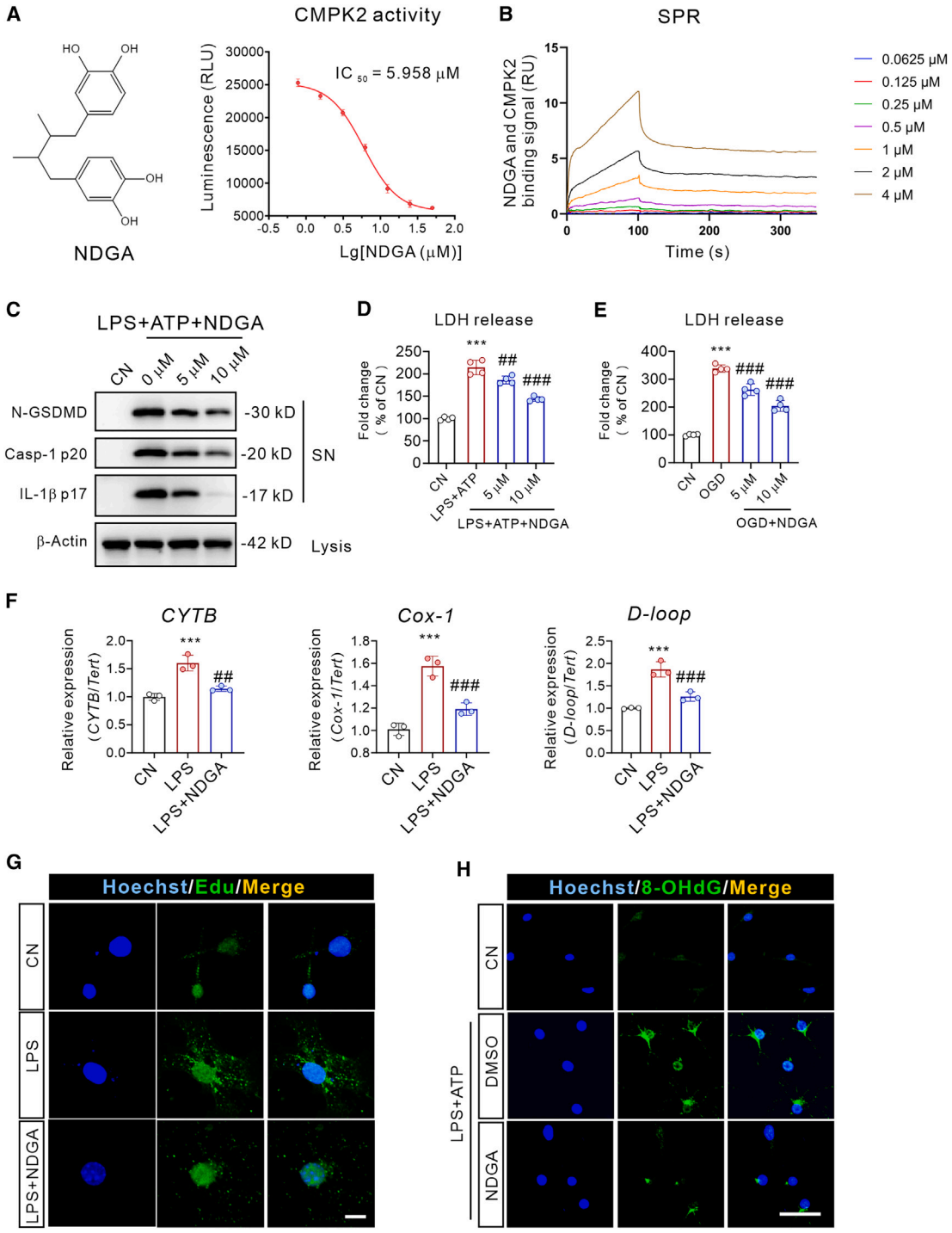

Figure 6. The CMPK2-specific inhibitor NDGA suppresses Ox-mtDNA formation and NLRP3 inflammasome activation in microglia *in vitro*

(A) The molecule structure of nordihydroguaiaretic acid (NDGA) and quantification of CMPK2 kinase assay with indicated concentrations of NDGA. $n = 3$.

(B) The real-time binding kinetics of NDGA to immobilized CMPK2 protein were examined by SPR assay with the K_D value of 0.6 μM.

(C) NDGA reduced the protein expression of cleaved caspase-1, N-GSDMD, and mature IL-1β in the cell supernatant of LPS-primed microglia cells followed by ATP stimulation.

(D and E) NDGA prevented LDH release in microglia subjected to LPS plus ATP stimulation or OGD model. $n = 4$. Results are represented as means ± SD. $^{***}p < 0.001$ vs. control (CN) group and $^{\#\#}p < 0.01$ and $^{\#\#\#}p < 0.001$ vs. LPS plus ATP or OGD group.

(legend continued on next page)

(Figures S7D and S7E). Hence, CMPK2 knockdown, followed by LPS plus ATP stimulation, could mitigate the mitochondrial fragmentation in primary mouse microglia cells.

Several studies have indicated that oxidative stress also enhances NLRP3 inflammasome activation[49–53]; thus, we investigated whether the inhibitory effects of CMPK2 knockdown on NLRP3 inflammasome activation were reliant on ROS generation. However, we found that CMPK2 knockdown did not change the level of mtROS production in primary microglial cells after LPS plus ATP stimulation (Figures S8A and S8B). The LPS-primed primary mouse microglia cells were treated with H_2O_2 for 6 h and then stimulated with ATP according to previous studies,[26,53,54] and we found that H_2O_2 administration failed to restore NLRP3 inflammasome activation in CMPK2-silenced microglia (Figures S8C and S8D). Furthermore, CMPK2 knockdown inhibited the colocalization of 8-OHdG with apoptosis-associated speck-like protein containing a CARD (ASC) specks in LPS-primed primary mouse microglia followed by ATP stimulation (Figures S8E and S8F). Hence, these findings indicated that CMPK2 knockdown may act by regulating Ox-mtDNA production, rather than ROS generation, to inhibit NLRP3 inflammasome activation in microglial cells.

Discovery of NDGA as a valid CMPK2 inhibitor with potent inhibitory effects on Ox-mtDNA formation and NLRP3 inflammasome activation *in vitro*

Based on above findings, we proposed that CMPK2 inhibitors may serve as promising pharmacological treatments for ischemic stroke. We screened compounds from compound library containing natural products and FDA-approved drugs and discovered that a natural compound, NDGA, was an effective CMPK2 inhibitor with a half-maximum inhibitory concentration of 5.958 μM (Figure 6A). NDGA is a plant lignan isolated from creosote bush and *Larrea* tridentata, usually discovered in North America and Mexico.[55] NDGA possesses pleiotropic effects, including anticancer, antioxidant, anti-inflammation, and analgesic activities.[55–57] Furthermore, as indicated by the surface plasmon resonance (SPR) results, there was a strong binding between NDGA and CMPK2 protein with a dissociation constant (K_D) value of 0.6 μM (Figure 6B). Therefore, we investigated whether NDGA could regulate NLRP3 inflammasome activation in microglia. As illustrated in Figures 6C and S9A, treatment with NDGA significantly inhibited the release of cleaved caspase-1, N-GSDMD, and mature IL-1β into cell supernatant in LPS-primed microglia followed by ATP stimulation. Then, we assessed the effects of NDGA on cell death in the LPS plus ATP or OGD-induced microglia cell injury model and found that NDGA could effectively tone down LDH release (Figures 6D and 6E). All the aforementioned suggested that NDGA could inhibit microglial pyroptosis *in vitro*. Inspired by these findings, we continued to seek out whether the effects of NDGA were associated with CMPK2 inhibition. As depicted by Figure 6F, NDGA treatment remarkably downregulated the expressions of *D-loop*, *Cox-1*, and *CYTB* in primary mouse microglia after LPS treatment. Also, the EdU staining results revealed that NDGA treatment remarkably reduced the newly synthesized mtDNA after LPS stimulation (Figure 6G and S9B). Additionally, the level of Ox-mtDNA was suppressed by NDGA treatment, as determined by 8-OHdG immunofluorescence staining in LPS-primed microglia followed by ATP stimulation (Figures 6H and S9C). Moreover, NDGA treatment greatly inhibited the newly synthesized mtDNA and Ox-mtDNA formation in the OGD-induced microglia injury model (Figures S9D–S9G). Then, we assessed the potential effects of NDGA treatment on mitochondrial functions, and the data showed that NDGA treatment did not change the ATP contents and could not rescue the reduction of PGC-1α and NRF1 expressions but effectively mitigated mitochondrial fragmentation in primary mouse microglia cells followed by LPS plus ATP stimulation (Figures S10A–S10E)

Previous literature has shown that NDGA is a valid lipoxygenase (LOX) inhibitor to elicit potent antioxidant actions.[55–57] To determine whether 5-LOX was crucial for the inhibitory effects of NDGA on the activation of the NLRP3 inflammasome, we knocked down 5-LOX using 5-LOX siRNA in primary mouse microglia cells (Figure S11A). As depicted in Figures S11B and S11C, 5-LOX knockdown did not impact the protein expression of cleaved caspase-1, N-GSDMD, or mature IL-1β in the cell supernatant of LPS-primed microglia followed by ATP stimulation. In addition, the inhibitory effects of NDGA on the release of cleaved caspase-1, N-GSDMD, and mature IL-1β were not influenced by 5-LOX silencing in microglia after LPS plus ATP stimulation (Figures S11B–S11C). In addition, NDGA treatment in CMPK2-silenced microglia did not produce more noticeable inhibitory effects on the release of cleaved caspase-1, N-GSDMD, and mature IL-1β in the cell supernatant of LPS-primed microglia followed by ATP stimulation (Figures S11D and S11E). Furthermore, H_2O_2, which further augmented the release of caspase-1, N-GSDMD, and mature IL-1β, cannot restore NLRP3 inflammasome activation in NDGA-treated microglia followed by LPS plus ATP stimulation (Figures S11F and S11G). These findings support the hypothesis that NDGA could suppress NLRP3 inflammasome activation primarily by inhibiting CMPK2 but not 5-LOX.

CMPK2 inhibitor NDGA elicits potent neuroprotective activity in the cerebral ischemic mice

Inspired by the above data, we examined the effects of NDGA in the mouse tMCAO model (Figures S12A–S12C). The CBF assessment indicated that there were no apparent differences in the CBF at baseline, during ischemia, or after reperfusion between the NDGA and vehicle groups (Figures S12D and S12E). Then, we discovered that NDGA administration dose-dependently ameliorated ischemic volume using TTC staining and markedly reduced neurological scores in the Longa test compared with the vehicle group after ischemia attack (Figures 7A–7C).

(F) NDGA decreased the *Cox-1*, *CYTB*, and *D-loop* expression in primary mouse microglia cells. $n = 3$. Results are represented as means ± SD. $^{***}p < 0.001$ vs. CN group and $^{\#\#}p < 0.01$ and $^{\#\#\#}p < 0.001$ vs. LPS group.
(G) NDGA reduced the newly synthesized DNA, as visualized by EdU labeling in primary mouse microglia cells. Scale bar: 5 μm. $n = 6$.
(H) NDGA reduced 8-OHdG expression in LPS-primed microglia followed by ATP stimulation. Scale bar: 20 μm. $n = 4$.

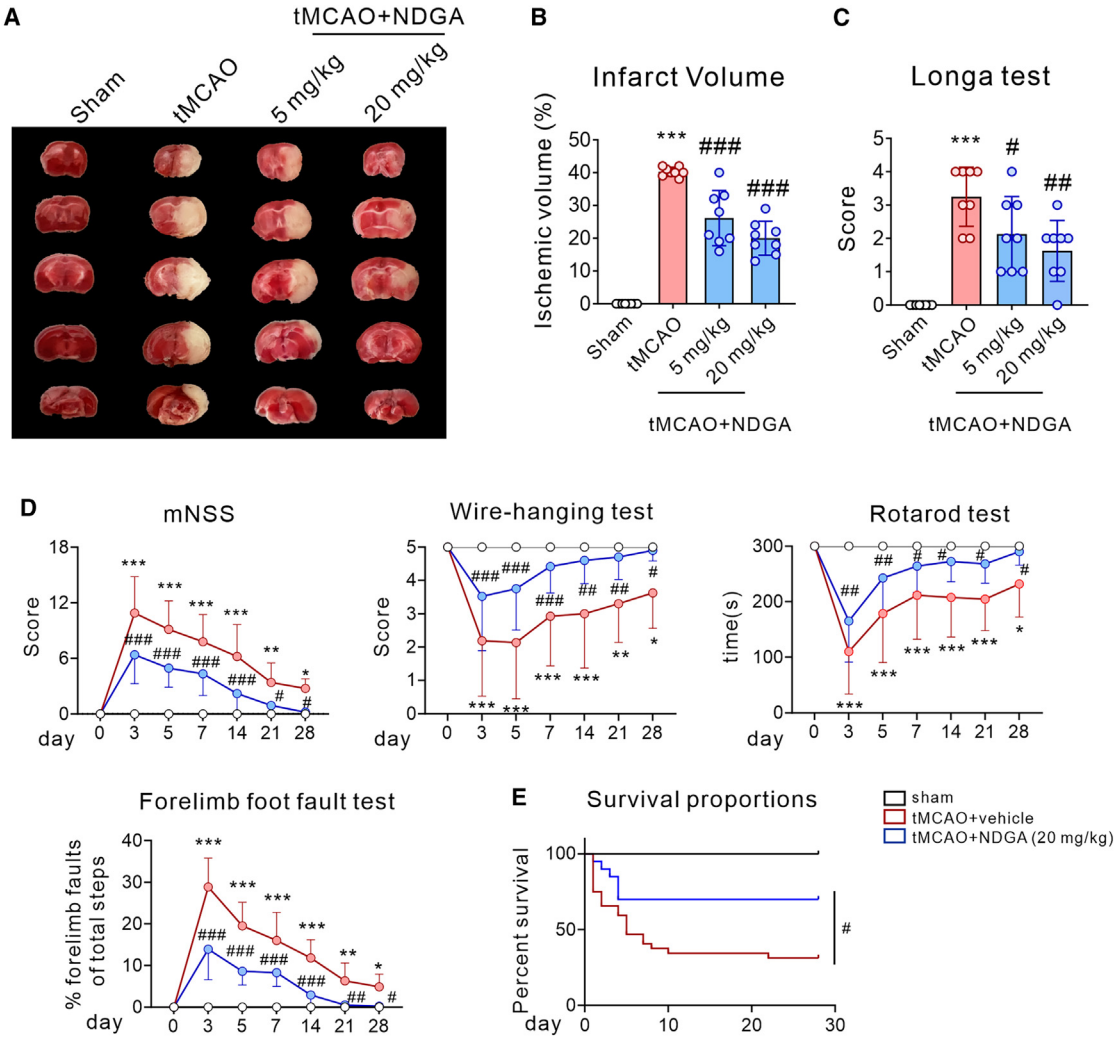

Figure 7. The CMPK2 inhibitor NDGA reduces brain ischemic volume and improves neurological performances in the mouse tMCAO model

(A–C) NDGA reduced cerebral infarct volume and promoted short-term neurological functions in the male mice. $n = 8$.

(D) NDGA improved long-term functional performances, including mNSS test, wire-hanging test, forelimb foot fault test, and rotarod test in the male mice. $n = 8$.

(E) NDGA improved long-term survival proportions in the male mice. $n = 12–15$.

Results are represented as means ± SD. $^{*}p < 0.05$, $^{**}p < 0.01$, and $^{***}p < 0.001$ vs. sham group and $^{\#}p < 0.05$, $^{\#\#}p < 0.01$, and $^{\#\#\#}p < 0.001$ vs. tMCAO plus vehicle group.

To explore whether the neuroprotective effects of NDGA in ischemic stroke were associated with CMPK2, we administrated AAV-shCon and AAV-shCMPK2 *CX$_3$CR1$^{Cre/ERT2}$* mice with an effective dosage of NDGA (20 mg/kg). As shown in Figures S12F–S12H, NDGA could not exhibit additional beneficial effects, including decreased ischemic lesion and enhanced short-term functional outcome, in AAV-shCMPK2 *CX$_3$CR1$^{Cre/ERT2}$* mice. Based on the above findings, we conclude that NDGA could effectively ameliorate ischemic brain injury in tMCAO mice mainly through CMPK2 inhibition.

In addition, the long-term functional performances were markedly improved with NDGA treatment in mice subjected to tMCAO, as indicated by the significantly decreased scores in the mNSS test, upregulated scores in the wire-hanging test, downregulated percentage of the forelimb faults in foot misteps, and increased time in the rotarod test relative to the vehicle group 0, 3, 5, 7, 14, 21, and 28 days post-ischemia (Figure 7D). Moreover, NDGA administration promoted the survival proportions at the relatively delayed stage (28 days) compared to the vehicle group in the mice post-ischemia (Figure 7E). These results indicated that NDGA could ameliorate ischemic damage and improve long-term neurological performances in mice subjected to ischemic stroke.

To better understand the mechanism underlying then neuroprotective effects of NDGA in ischemic stroke, we analyzed microglial morphological alterations using Iba1 immunofluorescent staining followed by 3D reconstruction. Evidently, administration of NDGA suppressed the hyperactivated state of microglia, as evidenced by increased process lengths and branches in comparison to the vehicle group following ischemic onset

(Figures S13A–S13C). Then, we investigated the effects of NDGA on Ox-mtDNA formation. Immunohistochemical staining analysis confirmed that NDGA substantially decreased 8-OHdG expression in microglia in the peri-infarct region of ischemic mice at 72 h after tMCAO compared with the vehicle group (Figures S13D and S13E). In addition, NDGA treatment greatly reduced the levels of cleaved caspase-1, N-GSDMD, and mature IL-1β in the peri-infarct region of ischemic mice at 72 h after tMCAO compared with the vehicle group (Figures S13F and S13G). Therefore, these data indicated that the NDGA could attenuate Ox-mtDNA formation and NLRP3 inflammasome activation in mice subjected to tMCAO.

CMPK2 inhibitor NDGA suppresses Ox-mtDNA production and NLPR3 inflammasome activation in primary human monocytes from patients with cerebral ischemic stroke

To corroborate the translational relevance of the findings from the *in vivo* and *in vitro* models described above, we further isolated the peripheral blood mononuclear cells (PBMCs) from patients with acute cerebral ischemic stroke and established the NLRP3 inflammasome activation model. Upon priming with LPS followed by ATP stimulation, mature IL-1β was substantially elevated in the cell supernatant of PBMCs (Figure S14A). Congruent with the above *in vitro* finding, NDGA treatment markedly inhibited IL-1β release (Figure S14A). Moreover, a positive correlation was observed between *CMPK2* gene expression and IL-1β inhibition rate by NDGA in PBMCs from patients with cerebral ischemic stroke (Figure S14B). We also examined the effects of NDGA on PBMCs from healthy donors and found that NDGA treatment could also inhibit mature IL-1β release after LPS plus ATP stimulation (Figure S14C). Additionally, NDGA treatment also mitigated Ox-mtDNA production in PBMCs, as determined by 8-OHdG immunofluorescence staining (Figures S14D and S14E). The aforementioned data support our hypothesis that NDGA, as a specific CMPK2 inhibitor, could limit Ox-mtDNA formation and NLRP3 inflammasome activation in primary human monocytes from patients with stroke and may have better therapeutic potential in patients with stroke with higher CMPK2 expression.

DISCUSSION

Currently, little is known about the potential role of CMPK2 in neuroinflammation and brain injury during ischemic stroke. Our study revealed that *Cre* recombination-dependent AAV-mediated microglia/macrophage CMPK2 knockdown or pharmacological intervention with NDGA mitigated ischemic injury by inhibiting Ox-mtDNA-induced NLRP3 inflammasome activation, indicating that microglial CMPK2 may play a crucial role in the pathological processes of ischemic stroke.

In the peripheral circulation system, Ox-mtDNA can act as one of the DAMPs to activate the NLRP3 inflammasome and then prompt the formation of GSDMD pores in the membranes of peripheral cells including monocytes, macrophages, and neutrophils, which allows the circulatory release of more Ox-mtDNA to initiate the inflammatory cascade.[14,26] Lorente et al. and Liu et al. also confirmed that concentrations of 8-OHdG were higher in the peripheral blood of ischemic patients and positively correlated with the severity of ischemic injury and poor prognosis.[18,58] Our data indicated that *CMPK2* gene expression in human stroke patients was positively correlated with infarct volume and NIHSS score, supporting the clinical significance of CMPK2 in ischemic stroke.

In peripheral system disorders, pharmacological interventions or gene knockout/knockdown of CMPK2 have demonstrated therapeutic effects on a series of inflammation-associated diseases, including ARDS, atherosclerosis, oral ulcer healing, and liver ischemia/reperfusion injury.[21–23,59] The sterile inflammation mediated by DAMPs is a crucial component in the pathophysiology after stroke; ATP, HMGB-1, MRP8 (S100A8), and MRP14 (S100A9) may be promising DAMPs to promote CMPK2 upregulation in the brain after stroke, which is worthy of further investigation. Nevertheless, the precise function of CMPK2 in neuroinflammation of central nervous system disorders remains elusive. Our experiments revealed that CMPK2 expression was substantially elevated in the peri-infarct region of ischemic rodents, predominantly located in the microglia. The *in vitro* data also supported the above finding that CMPK2 expression was markedly enhanced in microglia following OGD treatment. Consequently, our findings firmly suggested that microglia/macrophage CMPK2 expression was markedly increased in the peri-infarct region after cerebral ischemic attack.

In brain calcification, biallelic variants of CMPK2 lead to reduced mtDNA copies and promote mitochondrial dysfunction.[20] In addition, cannabidiol negatively regulates the transcriptional activity of PPARγ on CMPK2 and inhibits inflammasome activation, thereby relieving oral ulcer healing.[60] Moreover, myeloid-specific knockout of CMPK2 can mitigate pulmonary injury in ARDS.[21] Furthermore, CMPK2 accelerates the synthesis of deoxy-3′,4′-didehydro-cytidine triphosphate, blocking virus replication in CoVs.[24] However, the precise function of CMPK2 in microglia, particularly in the context of ischemic stroke, has not been investigated. Hence, we adopted a well-established strategy of AAV selective expression based on the *Cre* recombinase system to knock down CMPK2 expression in microglia. Microglia/macrophage CMPK2 silencing elicited protective effects in reducing ischemic volume and promoting short-term neurological outcome in ischemic mice at 3 days post-operation. Moreover, AAV-shCMPK2 injection attenuated long-term neurological deficits in the $CX_3CR1^{Cre/ERT2}$ mice, indicating that CMPK2 might be a biomarker associated with poor prognosis following stroke.

Microglia dynamically modulate the morphology between the ramified state and ameboid morphology, the latter of which indicates the activated state.[31] Although microglia of ameboid morphology help remove necrotic cells, cellular and myelin debris, and pathogens, prolonged exposure to hyperactivated microglia leads to neuron damage and loss. Our data demonstrated that CMPK2 knockdown maintained the homeostatic state of microglia, as indicated by increases in process lengths and branch number, which might enable microglia to react appropriately to an ischemic insult and enhance neurological performance. Han et al. also confirmed that enhanced microglial ramification mediated by PGC-1α protected against ischemia-induced brain injury in mice.[34] Cao et al. also highlighted the

essential role of microglia with a ramified morphology in surveillance and scavenging functions.[31] Therefore, we speculated that CMPK2 silencing would limit the overactivation of microglia, thus reducing brain infarct injury in the ischemic mice.

Under normal physiological conditions, mtDNA exists as a nucleoid with a compaction size of less than 5 μm, which is precisely regulated by the packaging and compaction of TFAM.[14,26] Under conditions of microbial infections, non-sterile inflammation, and tumor cell stimuli, mtDNA replication is extensively accelerated by CMPK2. Of note, the newly synthesized mtDNA is naked and unstable and can easily secrete into the cytosol through mPTP and VDAC1, thereby exacerbating tissue injury.[14] Especially, the D-loop bubble of mtDNA is vulnerable to oxidative stress and then is oxidized by ROSs to produce Ox-mtDNA, which can directly activate the NLRP3 inflammasome. Furthermore, microglial Hv1 increases ROS generation through NADPH oxidase regulation and then aggravates neuron death and brain injury after neurological disorders,[61–65] which may synergize with CMPK2 to exacerbate neuroinflammation and neuron death after ischemic stroke. Our current study showed that CMPK2 knockdown suppressed new mtDNA synthesis, as determined by EdU staining, inhibited levels of representative mtDNA markers, including D-loop, *Cox1*, and *CYTB*, and disrupted Ox-mtDNA formation, as determined by 8-OHdG immunofluorescence staining in primary mouse microglia upon LPS priming followed by ATP stimulation or OGD conditions *in vitro*. The *in vivo* data also validated that CMPK2 knockdown inhibited 8-OHdG expression in microglia/macrophages in the ischemic mice stroke model. Furthermore, CMPK2 silencing inhibited cleaved caspase-1, mature IL-1β, and bioactive N-GSDMD in the mouse tMCAO model *in vivo* and LPS-primed microglia followed by ATP stimulation *in vitro*. Xian et al. also verified that myeloid-specific CMPK2 ablation suppressed IL-1β production and NLRP3 inflammasome assembly in LPS-induced ARDS.[20] Zhong et al. highlighted that mtDNA and 8-OHdG, rather than mtROSs, directly enabled NLRP3 inflammasome activation.[25] Thus, we concluded that CMPK2 accelerated mtDNA replication and Ox-mtDNA production and then promoted NLRP3 inflammasome activation in the microglia so as to aggravate the brain injury after ischemic stroke.

Target identification and lead discovery are critical steps in drug discovery for clinical use. Using the CMPK2 kinase assay combined with the SPR assay, we identified NDGA as a potent CMPK2 inhibitor. NDGA is the principal metabolite of creosote bush and has been confirmed as a promising agent for treating multiple diseases, including cardiovascular diseases, neurological disorders, and cancers, as well as viral infections.[55–57] In addition, a previous investigation reported that NDGA ameliorated cerebral infarction volume by inhibiting neuronal apoptosis in a rat with ischemic stroke, but the cellular and molecular mechanisms underlying the neuroprotective effects of NDGA remain ambiguous under ischemia stimuli.[55–57] Therefore, a deeper understanding of the precise mechanisms of NDGA in microglia will help explain its therapeutic efficacy and lead to the discovery of NDGA derivatives with enhanced therapeutic potential for ischemic stroke. Our data revealed that NDGA treatment blocked the new mtDNA synthesis and inhibited 8-OHdG formation, corroborating the abovementioned findings that CMPK2 knockdown could efficiently suppress mtDNA replication and Ox-mtDNA production. In addition, NDGA treatment could potently reduce the levels of cleaved caspase-1, mature IL-1β, and bioactive N-GSDMD in LPS-primed microglia followed by ATP stimulation *in vitro* and the mouse tMCAO model *in vivo*. However, 5-LOX knockdown could not diminish the protein expressions of cleaved caspase-1, mature IL-1β, or bioactive N-GSDMD, nor could it influence the inhibitory effects of NDGA on NLRP3 inflammasome in LPS-primed microglia following ATP stimulation. Moreover, NDGA treatment had no further suppressive effects on NLRP3 inflammasome activation in CMPK2-silenced microglia. These findings indicated that the role of NDGA in NLRP3 inflammasome activation was independent of 5-LOX but at least partially dependent on CMPK2. Furthermore, we also observed that NDGA reduced ischemic volume and short-term and long-term neurological deficits in the mouse tMCAO model. Subsequently, we studied whether the neuroprotective effects of NDGA were correlated with CMPK2. Our data proved that NDGA cannot produce additional therapeutic effects in AAV-shCMPK2 $CX_3CR1^{Cre/ERT2}$ mice after ischemic stroke, which validated that the neuroprotective effects of NDGA in ischemic stroke were at least partially dependent on CMPK2. To better ascertain the clinical relevance of CMPK2, we evaluated the effects of CMPK2-specific inhibitor NDGA on primary human monocytes. We discovered that NDGA substantially reduced mature IL-1β release and 8-OHdG expression in LPS-primed PBMCs, followed by ATP stimulation. Of note, we observed a positive correlation between *CMPK2* gene expression and IL-1β inhibition rate by NDGA, indicating that CMPK2 expression was highly associated with the inhibition rate of NDGA on CMPK2. In conclusion, NDGA administration, a promising immunotherapy based on CMPK2 inhibition, promises to be a mainstay of ischemic stroke management in future clinical research.

Limitations of the study

There are several unsolved issues in the current investigation. First, we confirmed that microglia CMPK2 knockdown ameliorates cerebral ischemic injury by inhibiting the Ox-mtDNA-induced NLRP3 inflammasome activation. However, it cannot be ruled out that other mechanisms of CMPK2 action besides the NLRP3 inflammasome may contribute to the progression of ischemic stroke. Specifically, it remains to be determined whether the STING signaling pathway is involved in the function of CMPK2 in cerebral ischemic injury. Second, the signaling pathways or key mediators that promote the increase of CMPK2 protein remain obscure, so further experimental and rodent models (microglia CMPK2 transgenic or knockout mice) are required. Third, neuroinflammation is implicated in a series of disease processes, including Alzheimer's disease, vascular dementia, traumatic brain injury, and multiple sclerosis. We will further continue to explore whether CMPK2 participates in other neurologic disorders, such as multiple sclerosis and vascular dementia. Fourth, due to the unavailability of human brain samples and primary human microglia from patients with stroke, we obtained primary human monocytes isolated from patients with stroke to evaluate the inhibitory effects of CMPK2-specific inhibitor NDGA on NLRP3 inflammasome activation *in vitro*. Thus, our

understanding of CMPK2 function in patients with ischemic stroke is less refined. Hence, human postmortem brain tissue may be utilized in our ongoing research. Lastly, the brain tissue of rodents and humans differs greatly; therefore, non-human primates would be an alternative model to evaluate the role of CMPK2 in ischemic stroke through pharmacological modulation and genetic intervention. Nevertheless, our findings in this study would provide CMPK2 as a potential target for ischemic stroke and also CMPK2 inhibitor NDGA as a valuable therapeutic agent for the treatment of ischemic stroke.

STAR★METHODS

Detailed methods are provided in the online version of this paper and include the following:

- KEY RESOURCES TABLE
- RESOURCE AVAILABILITY
  - Lead contact
  - Materials availability
  - Data and code availability
- EXPERIMENTAL MODEL AND SUBJECT DETAILS
  - Human sample collection and processing
  - Animals
  - Isolation of primary mouse cortical neurons, astrocytes and microglia
- METHOD DETAILS
  - Quantitative real-time PCR (qRT-PCR)
  - Western blotting analysis
  - CMPK2 protein and antibody production
  - Establishment of focal cerebral ischemia/reperfusion model
  - Assessment of cerebral infarct volume and neurological function
  - Immunofluorescence staining
  - Adult mouse microglial isolation and flow cytometry examination
  - Oxygen-glucose deprivation (OGD) treatment
  - Stereotaxic surgery
  - *In vivo* mouse brain magnetic resonance imaging (MRI) scanning
  - Three-dimensional (3D) reconstruction
  - LPS-primed NLRP3 inflammasome model in primary mouse microglia cells and human primary monocytes
  - Cell transfection
  - Analysis of lactate dehydrogenase (LDH) release
  - Edu staining experiment
  - Measurement of total mtDNA
  - Enzyme-linked immunosorbent assay (ELISA) for IL-1β cytokine
  - *In vitro* CMPK2 kinase assay and compounds screening
  - Surface plasmon resonance (SPR) assay
- QUANTIFICATION AND STATISTICAL ANALYSIS

SUPPLEMENTAL INFORMATION

Supplemental information can be found online at https://doi.org/10.1016/j.xcrm.2024.101522.

ACKNOWLEDGMENTS

This work was supported by the National Natural Science Foundation of China (82174010, 81973512, and 81973500); The Open Fund of the State Key Laboratory of Pharmaceutical Biotechnology, Nanjing University, China (grant no. KF-202206), and the Double First-Class Project of China Pharmaceutical University (CPUQNJC22_02).

AUTHOR CONTRIBUTIONS

T.P., X.X., J.W., and X.G. conceived the project and designed the studies. X.G., J.W., and T.P. wrote the paper. M.L. and Y.W. collected human samples. S.Z. performed enzyme assay and compound screening. X.G., J.S., K.L., and L.X. revised the manuscript. X.G., J.S., K.L., and L.X. conducted animal experiments. X.G., J.S., and K.L. performed the molecular biology and cell biology experiments.

DECLARATION OF INTERESTS

The authors declare no competing interests.

Received: October 29, 2023
Revised: February 8, 2024
Accepted: March 28, 2024
Published: April 26, 2024

REFERENCES

1. Owolabi, M.O., Thrift, A.G., Mahal, A., Ishida, M., Martins, S., Johnson, W.D., Pandian, J., Abd-Allah, F., Yaria, J., Phan, H.T., et al. (2022). Primary stroke prevention worldwide: translating evidence into action. Lancet Public Health *7*, e74–e85. https://doi.org/10.1016/S2468-2667(21)00230-9.
2. Yu, H., Chen, X., Guo, X., Chen, D., Jiang, L., Qi, Y., Shao, J., Tao, L., Hang, J., Lu, G., et al. (2023). The clinical value of serum xanthine oxidase levels in patients with acute ischemic stroke. Redox Biol. *60*, 102623. https://doi.org/10.1016/j.redox.2023.102623.
3. Barclay, R.E., Stevenson, T.J., Poluha, W., Semenko, B., and Schubert, J. (2020). Mental practice for treating upper extremity deficits in individuals with hemiparesis after stroke. Cochrane Database Syst. Rev. *5*, CD005950. https://doi.org/10.1002/14651858.CD005950.pub5.
4. (2021). Global, regional, and national burden of stroke and its risk factors, 1990-2019: a systematic analysis for the Global Burden of Disease Study 2019. Lancet Neurol. *20*, 795–820. https://doi.org/10.1016/S1474-4422(21)00252-0.
5. Wang, R., Zhu, Y., Liu, Z., Chang, L., Bai, X., Kang, L., Cao, Y., Yang, X., Yu, H., Shi, M.-J., et al. (2021). Neutrophil extracellular traps promote tPA-induced brain hemorrhage via cGAS in mice with stroke. Blood *138*, 91–103. https://doi.org/10.1182/blood.2020008913.
6. Brenna, S., Altmeppen, H.C., Mohammadi, B., Rissiek, B., Schlink, F., Ludewig, P., Krisp, C., Schlüter, H., Failla, A.V., Schneider, C., et al. (2020). Characterization of brain-derived extracellular vesicles reveals changes in cellular origin after stroke and enrichment of the prion protein with a potential role in cellular uptake. J. Extracell. Vesicles *9*, 1809065. https://doi.org/10.1080/20013078.2020.1809065.
7. Loppi, S., Korhonen, P., Bouvy-Liivrand, M., Caligola, S., Turunen, T.A., Turunen, M.P., Hernandez de Sande, A., Kołosowska, N., Scoyni, F., Rosell, A., et al. (2021). Peripheral inflammation preceeding ischemia impairs neuronal survival through mechanisms involving miR-127 in aged animals. Aging Cell *20*, e13287. https://doi.org/10.1111/acel.13287.
8. Guan, X., Wu, J., Geng, J., Ji, D., Wei, D., Ling, Y., Zhang, Y., Jiang, G., Pang, T., and Huang, Z. (2024). A Novel Hybrid of Telmisartan and Borneol Ameliorates Neuroinflammation and White Matter Injury in Ischemic Stroke Through ATF3/CH25H Axis. Transl. Stroke Res. *15*, 195–218. https://doi.org/10.1007/s12975-022-01121-5.
9. Paolicelli, R.C., Sierra, A., Stevens, B., Tremblay, M.-E., Aguzzi, A., Ajami, B., Amit, I., Audinat, E., Bechmann, I., Bennett, M., et al. (2022). Microglia states and nomenclature: A field at its crossroads. Neuron *110*, 3458–3483. https://doi.org/10.1016/j.neuron.2022.10.020.
10. Kim, S., Lee, W., Jo, H., Sonn, S.-K., Jeong, S.-J., Seo, S., Suh, J., Jin, J., Kweon, H.Y., Kim, T.K., et al. (2022). The antioxidant enzyme Peroxiredoxin-1 controls stroke-associated microglia against acute ischemic stroke. Redox Biol. *54*, 102347. https://doi.org/10.1016/j.redox.2022.102347.

11. Bernhart, E., Kogelnik, N., Prasch, J., Gottschalk, B., Goeritzer, M., Depaoli, M.R., Reicher, H., Nusshold, C., Plastira, I., Hammer, A., et al. (2018). 2-Chlorohexadecanoic acid induces ER stress and mitochondrial dysfunction in brain microvascular endothelial cells. Redox Biol. *15*, 441–451. https://doi.org/10.1016/j.redox.2018.01.003.

12. Kotrys, A.V., Cysewski, D., Czarnomska, S.D., Pietras, Z., Borowski, L.S., Dziembowski, A., and Szczesny, R.J. (2019). Quantitative proteomics revealed C6orf203/MTRES1 as a factor preventing stress-induced transcription deficiency in human mitochondria. Nucleic Acids Res. *47*, 7502–7517. https://doi.org/10.1093/nar/gkz542.

13. Kosmider, B., Lin, C.-R., Karim, L., Tomar, D., Vlasenko, L., Marchetti, N., Bolla, S., Madesh, M., Criner, G.J., and Bahmed, K. (2019). Mitochondrial dysfunction in human primary alveolar type II cells in emphysema. EBioMedicine *46*, 305–316. https://doi.org/10.1016/j.ebiom.2019.07.063.

14. Xian, H., and Karin, M. (2023). Oxidized mitochondrial DNA: a protective signal gone awry. Trends Immunol. *44*, 188–200. https://doi.org/10.1016/j.it.2023.01.006.

15. Hsieh, Y.-W., Lin, K.-C., Korivi, M., Lee, T.-H., Wu, C.-Y., and Wu, K.-Y. (2014). The reliability and predictive ability of a biomarker of oxidative DNA damage on functional outcomes after stroke rehabilitation. Int. J. Mol. Sci. *15*, 6504–6516. https://doi.org/10.3390/ijms15046504.

16. Liu, Z., Liu, Y., Tu, X., Shen, H., Qiu, H., Chen, H., and He, J. (2017). High Serum Levels of Malondialdehyde and 8-OHdG are both Associated with Early Cognitive Impairment in Patients with Acute Ischaemic Stroke. Sci. Rep. *7*, 9493. https://doi.org/10.1038/s41598-017-09988-3.

17. Nakajima, H., Unoda, K.-I., Ito, T., Kitaoka, H., Kimura, F., and Hanafusa, T. (2012). The Relation of Urinary 8-OHdG, A Marker of Oxidative Stress to DNA, and Clinical Outcomes for Ischemic Stroke. Open Neurol. J. *6*, 51–57. https://doi.org/10.2174/1874205X01206010051.

18. Liu, Z., Cai, Y., and He, J. (2018). High serum levels of 8-OHdG are an independent predictor of post-stroke depression in Chinese stroke survivors. Neuropsychiatr. Dis. Treat. *14*, 587–596. https://doi.org/10.2147/NDT.S155144.

19. Mizukoshi, G., Katsura, K.-I., and Katayama, Y. (2005). Urinary 8-hydroxy-2'-deoxyguanosine and serum S100beta in acute cardioembolic stroke patients. Neurol. Res. *27*, 644–646.

20. Zhao, M., Su, H.-Z., Zeng, Y.-H., Sun, Y., Guo, X.-X., Li, Y.-L., Wang, C., Zhao, Z.-Y., Huang, X.-J., Lin, K.-J., et al. (2022). Loss of function of CMPK2 causes mitochondria deficiency and brain calcification. Cell Discov. *8*, 128. https://doi.org/10.1038/s41421-022-00475-2.

21. Xian, H., Liu, Y., Rundberg Nilsson, A., Gatchalian, R., Crother, T.R., Tourtellotte, W.G., Zhang, Y., Aleman-Muench, G.R., Lewis, G., Chen, W., et al. (2021). Metformin inhibition of mitochondrial ATP and DNA synthesis abrogates NLRP3 inflammasome activation and pulmonary inflammation. Immunity *54*, 1463–1477.e11. https://doi.org/10.1016/j.immuni.2021.05.004.

22. Chen, Y., Wu, L., Shi, M., Zeng, D., Hu, R., Wu, X., Han, S., He, K., Xu, H., Shao, X., and Ma, R. (2022). Electroacupuncture Inhibits NLRP3 Activation by Regulating CMPK2 After Spinal Cord Injury. Front. Immunol. *13*, 788556. https://doi.org/10.3389/fimmu.2022.788556.

23. Pawlak, J.B., Hsu, J.C.-C., Xia, H., Han, P., Suh, H.-W., Grove, T.L., Morrison, J., Shi, P.-Y., Cresswell, P., and Laurent-Rolle, M. (2023). CMPK2 restricts Zika virus replication by inhibiting viral translation. PLoS Pathog. *19*, e1011286. https://doi.org/10.1371/journal.ppat.1011286.

24. Zhu, M., Lv, J., Wang, W., Guo, R., Zhong, C., Antia, A., Zeng, Q., Li, J., Liu, Q., Zhou, J., et al. (2023). CMPK2 is a host restriction factor that inhibits infection of multiple coronaviruses in a cell-intrinsic manner. PLoS Biol. *21*, e3002039. https://doi.org/10.1371/journal.pbio.3002039.

25. Newman, L.E., and Shadel, G.S. (2023). Mitochondrial DNA Release in Innate Immune Signaling. Annu. Rev. Biochem. *92*, 299–332. https://doi.org/10.1146/annurev-biochem-032620-104401.

26. Zhong, Z., Liang, S., Sanchez-Lopez, E., He, F., Shalapour, S., Lin, X.-J., Wong, J., Ding, S., Seki, E., Schnabl, B., et al. (2018). New mitochondrial DNA synthesis enables NLRP3 inflammasome activation. Nature *560*, 198–203. https://doi.org/10.1038/s41586-018-0372-z.

27. Tang, Y., Xu, H., Du, X., Lit, L., Walker, W., Lu, A., Ran, R., Gregg, J.P., Reilly, M., Pancioli, A., et al. (2006). Gene expression in blood changes rapidly in neutrophils and monocytes after ischemic stroke in humans: a microarray study. J. Cerebr. Blood Flow Metabol. *26*, 1089–1102.

28. Raman, K., O'Donnell, M.J., Czlonkowska, A., Duarte, Y.C., Lopez-Jaramillo, P., Peñaherrera, E., Sharma, M., Shoamanesh, A., Skowronska, M., Yusuf, S., and Paré, G. (2016). Peripheral Blood MCEMP1 Gene Expression as a Biomarker for Stroke Prognosis. Stroke *47*, 652–658. https://doi.org/10.1161/STROKEAHA.115.011854.

29. Zhang, J., Wang, C., Chen, X., Takada, M., Fan, C., Zheng, X., Wen, H., Liu, Y., Wang, C., Pestell, R.G., et al. (2015). EglN2 associates with the NRF1-PGC1α complex and controls mitochondrial function in breast cancer. EMBO J. *34*, 2953–2970. https://doi.org/10.15252/embj.201591437.

30. West, A.P., Khoury-Hanold, W., Staron, M., Tal, M.C., Pineda, C.M., Lang, S.M., Bestwick, M., Duguay, B.A., Raimundo, N., MacDuff, D.A., et al. (2015). Mitochondrial DNA stress primes the antiviral innate immune response. Nature *520*, 553–557. https://doi.org/10.1038/nature14156.

31. Cao, P., Chen, C., Liu, A., Shan, Q., Zhu, X., Jia, C., Peng, X., Zhang, M., Farzinpour, Z., Zhou, W., et al. (2021). Early-life inflammation promotes depressive symptoms in adolescence via microglial engulfment of dendritic spines. Neuron *109*, 2573–2589.e9. https://doi.org/10.1016/j.neuron.2021.06.012.

32. Harrington, J.S., Ryter, S.W., Plataki, M., Price, D.R., and Choi, A.M.K. (2023). Mitochondria in health, disease, and aging. Physiol. Rev. *103*, 2349–2422. https://doi.org/10.1152/physrev.00058.2021.

33. Studer, B., Timm, A., Sahakian, B.J., Kalenscher, T., and Knecht, S. (2021). A decision-neuroscientific intervention to improve cognitive recovery after stroke. Brain *144*, 1764–1773. https://doi.org/10.1093/brain/awab128.

34. Han, B., Jiang, W., Cui, P., Zheng, K., Dang, C., Wang, J., Li, H., Chen, L., Zhang, R., Wang, Q.M., et al. (2021). Microglial PGC-1α protects against ischemic brain injury by suppressing neuroinflammation. Genome Med. *13*, 47. https://doi.org/10.1186/s13073-021-00863-5.

35. Li, D., Lang, W., Zhou, C., Wu, C., Zhang, F., Liu, Q., Yang, S., and Hao, J. (2018). Upregulation of Microglial ZEB1 Ameliorates Brain Damage after Acute Ischemic Stroke. Cell Rep. *22*, 3574–3586. https://doi.org/10.1016/j.celrep.2018.03.011.

36. Gu, N., Peng, J., Murugan, M., Wang, X., Eyo, U.B., Sun, D., Ren, Y., DiCicco-Bloom, E., Young, W., Dong, H., and Wu, L.-J. (2016). Spinal Microgliosis Due to Resident Microglial Proliferation Is Required for Pain Hypersensitivity after Peripheral Nerve Injury. Cell Rep. *16*, 605–614. https://doi.org/10.1016/j.celrep.2016.06.018.

37. Zhang, C.-J., Jiang, M., Zhou, H., Liu, W., Wang, C., Kang, Z., Han, B., Zhang, Q., Chen, X., Xiao, J., et al. (2018). TLR-stimulated IRAKM activates caspase-8 inflammasome in microglia and promotes neuroinflammation. J. Clin. Invest. *128*, 5399–5412. https://doi.org/10.1172/JCI121901.

38. McDonough, A., Noor, S., Lee, R.V., Dodge, R., Strosnider, J.S., Shen, J., Davidson, S., Möller, T., Garden, G.A., and Weinstein, J.R. (2020). Ischemic preconditioning induces cortical microglial proliferation and a transcriptomic program of robust cell cycle activation. Glia *68*, 76–94. https://doi.org/10.1002/glia.23701.

39. Walsh, J.G., Muruve, D.A., and Power, C. (2014). Inflammasomes in the CNS. Nat. Rev. Neurosci. *15*, 84–97. https://doi.org/10.1038/nrn3638.

40. Chen, S., Mei, S., Luo, Y., Wu, H., Zhang, J., and Zhu, J. (2018). Gasdermin Family: a Promising Therapeutic Target for Stroke. Transl. Stroke Res. *9*, 555–563. https://doi.org/10.1007/s12975-018-0666-3.

41. He, M., Chiang, H.-H., Luo, H., Zheng, Z., Qiao, Q., Wang, L., Tan, M., Ohkubo, R., Mu, W.-C., Zhao, S., et al. (2020). An Acetylation Switch of the NLRP3 Inflammasome Regulates Aging-Associated Chronic Inflammation and Insulin Resistance. Cell Metabol. *31*, 580–591.e5. https://doi.org/10.1016/j.cmet.2020.01.009.

42. Han, X., Xu, T., Fang, Q., Zhang, H., Yue, L., Hu, G., and Sun, L. (2021). Quercetin hinders microglial activation to alleviate neurotoxicity via the interplay between NLRP3 inflammasome and mitophagy. Redox Biol. *44*, 102010. https://doi.org/10.1016/j.redox.2021.102010.

43. Li, S., Fang, Y., Zhang, Y., Song, M., Zhang, X., Ding, X., Yao, H., Chen, M., Sun, Y., Ding, J., et al. (2022). Microglial NLRP3 inflammasome activates neurotoxic astrocytes in depression-like mice. Cell Rep. *41*, 111532. https://doi.org/10.1016/j.celrep.2022.111532.

44. Ding, L., Yang, X., Tian, H., Liang, J., Zhang, F., Wang, G., Wang, Y., Ding, M., Shui, G., and Huang, X. (2018). Seipin regulates lipid homeostasis by ensuring calcium-dependent mitochondrial metabolism. EMBO J. *37*, e97572. https://doi.org/10.15252/embj.201797572.

45. Yu, B., Ma, J., Li, J., Wang, D., Wang, Z., and Wang, S. (2020). Mitochondrial phosphatase PGAM5 modulates cellular senescence by regulating mitochondrial dynamics. Nat. Commun. *11*, 2549. https://doi.org/10.1038/s41467-020-16312-7.

46. Huang, T., Lin, R., Su, Y., Sun, H., Zheng, X., Zhang, J., Lu, X., Zhao, B., Jiang, X., Huang, L., et al. (2023). Efficient intervention for pulmonary fibrosis via mitochondrial transfer promoted by mitochondrial biogenesis. Nat. Commun. *14*, 5781. https://doi.org/10.1038/s41467-023-41529-7.

47. Zhao, T., Zhang, J., Lei, H., Meng, Y., Cheng, H., Zhao, Y., Geng, G., Mu, C., Chen, L., Liu, Q., et al. (2023). NRF1-mediated mitochondrial biogenesis antagonizes innate antiviral immunity. EMBO J. *42*, e113258. https://doi.org/10.15252/embj.2022113258.

48. Zeng, Z., You, M., Fan, C., Rong, R., Li, H., and Xia, X. (2023). Pathologically high intraocular pressure induces mitochondrial dysfunction through Drp1 and leads to retinal ganglion cell PANoptosis in glaucoma. Redox Biol. *62*, 102687. https://doi.org/10.1016/j.redox.2023.102687.

49. Chen, J., Sun, W., Zhang, H., Ma, J., Xu, P., Yu, Y., Fang, H., Zhou, L., Lv, J., Xie, J., et al. (2020). Macrophages reprogrammed by lung cancer microparticles promote tumor development via release of IL-1β. Cell. Mol. Immunol. *17*, 1233–1244. https://doi.org/10.1038/s41423-019-0313-2.

50. Muñoz-Wolf, N., Ward, R.W., Hearnden, C.H., Sharp, F.A., Geoghegan, J., O'Grady, K., McEntee, C.P., Shanahan, K.A., Guy, C., Bowie, A.G., et al. (2023). Non-canonical inflammasome activation mediates the adjuvanticity of nanoparticles. Cell Rep. Med. *4*, 100899. https://doi.org/10.1016/j.xcrm.2022.100899.

51. Jin, X., Liu, D., Zhou, X., Luo, X., Huang, Q., and Huang, Y. (2023). Entrectinib inhibits NLRP3 inflammasome and inflammatory diseases by directly targeting NEK7. Cell Rep. Med. *4*, 101310. https://doi.org/10.1016/j.xcrm.2023.101310.

52. Sidor, K., Jeznach, A., Hoser, G., and Skirecki, T. (2023). 1-Methylnicotinamide (1-MNA) inhibits the activation of the NLRP3 inflammasome in human macrophages. Int. Immunopharm. *121*, 110445. https://doi.org/10.1016/j.intimp.2023.110445.

53. Bai, H., Yang, B., Yu, W., Xiao, Y., Yu, D., and Zhang, Q. (2018). Cathepsin B links oxidative stress to the activation of NLRP3 inflammasome. Exp. Cell Res. *362*, 180–187. https://doi.org/10.1016/j.yexcr.2017.11.015.

54. Rajanbabu, V., Galam, L., Fukumoto, J., Enciso, J., Tadikonda, P., Lane, T.N., Bandyopadhyay, S., Parthasarathy, P.T., Cho, Y., Cho, S.H., et al. (2015). Genipin suppresses NLRP3 inflammasome activation through uncoupling protein-2. Cell. Immunol. *297*, 40–45. https://doi.org/10.1016/j.cellimm.2015.06.002.

55. Liu, Y., Wang, H., Zhu, Y., Chen, L., Qu, Y., and Zhu, Y. (2012). The protective effect of nordihydroguaiaretic acid on cerebral ischemia/reperfusion injury is mediated by the JNK pathway. Brain Res. *1445*, 73–81. https://doi.org/10.1016/j.brainres.2012.01.031.

56. Shishido, Y., Furushiro, M., Hashimoto, S., and Yokokura, T. (2001). Effect of nordihydroguaiaretic acid on behavioral impairment and neuronal cell death after forebrain ischemia. Pharmacol. Biochem. Behav. *69*, 469–474.

57. Aktan, S., Aykut, C., Yegen, B.C., Okar, I., Ozkutlu, U., and Ercan, S. (1993). The effect of nordihydroguaiaretic acid on leukotriene C4 and prostaglandin E2 production following different reperfusion periods in rat brain after forebrain ischemia correlated with morphological changes. Prostaglandins Leukot. Essent. Fatty Acids *49*, 633–641.

58. Lorente, L., Martín, M.M., González-Rivero, A.F., Pérez-Cejas, A., Abreu-González, P., Ramos, L., Argueso, M., Cáceres, J.J., Solé-Violán, J., Alvarez-Castillo, A., et al. (2021). DNA and RNA oxidative damage are associated to mortality in patients with cerebral infarction. Med. Intensiva *45*, 35–41. https://doi.org/10.1016/j.medin.2019.07.008.

59. Wu, W., Bao, W., Chen, X., Lu, Y., Fang, J., Liu, J., Peng, S., Pi, J., Tomlinson, B., Chan, P., et al. (2023). Endothelial Gata6 deletion reduces monocyte recruitment and proinflammatory macrophage formation and attenuates atherosclerosis through Cmpk2-Nlrp3 pathways. Redox Biol. *64*, 102775. https://doi.org/10.1016/j.redox.2023.102775.

60. Qi, X., Lin, W., Wu, Y., Li, Q., Zhou, X., Li, H., Xiao, Q., Wang, Y., Shao, B., and Yuan, Q. (2022). CBD Promotes Oral Ulcer Healing via Inhibiting CMPK2-Mediated Inflammasome. J. Dent. Res. *101*, 206–215. https://doi.org/10.1177/00220345211024528.

61. Wu, L.-J. (2014). Microglial voltage-gated proton channel Hv1 in ischemic stroke. Transl. Stroke Res. *5*, 99–108. https://doi.org/10.1007/s12975-013-0289-7.

62. Wu, L.-J., Wu, G., Akhavan Sharif, M.R., Baker, A., Jia, Y., Fahey, F.H., Luo, H.R., Feener, E.P., and Clapham, D.E. (2012). The voltage-gated proton channel Hv1 enhances brain damage from ischemic stroke. Nat. Neurosci. *15*, 565–573. https://doi.org/10.1038/nn.3059.

63. Liu, X., Lei, Z., Gilhooly, D., He, J., Li, Y., Ritzel, R.M., Li, H., Wu, L.-J., Liu, S., and Wu, J. (2023). Traumatic brain injury-induced inflammatory changes in the olfactory bulb disrupt neuronal networks leading to olfactory dysfunction. Brain Behav. Immun. *114*, 22–45. https://doi.org/10.1016/j.bbi.2023.08.004.

64. Haruwaka, K., Ying, Y., Liang, Y., Umpierre, A.D., Yi, M.-H., Kremen, V., Chen, T., Xie, T., Qi, F., Zhao, S., et al. (2024). Microglia enhance postanesthesia neuronal activity by shielding inhibitory synapses. Nat. Neurosci. *27*, 449–461. https://doi.org/10.1038/s41593-023-01537-8.

65. Zhao, S., Umpierre, A.D., and Wu, L.-J. (2024). Tuning neural circuits and behaviors by microglia in the adult brain. Trends Neurosci. *47*, 181–194. https://doi.org/10.1016/j.tins.2023.12.003.

66. He, T., Shang, J., Gao, C., Guan, X., Chen, Y., Zhu, L., Zhang, L., Zhang, C., Zhang, J., and Pang, T. (2021). A novel SIRT6 activator ameliorates neuroinflammation and ischemic brain injury via EZH2/FOXC1 axis. Acta Pharm. Sin. B *11*, 708–726. https://doi.org/10.1016/j.apsb.2020.11.002.

67. Iiott, N.E., Heward, J.A., Roux, B., Tsitsiou, E., Fenwick, P.S., Lenzi, L., Goodhead, I., Hertz-Fowler, C., Heger, A., Hall, N., et al. (2014). Long non-coding RNAs and enhancer RNAs regulate the lipopolysaccharide-induced inflammatory response in human monocytes. Nat. Commun. *5*, 3979. https://doi.org/10.1038/ncomms4979.

68. Jin, M., Shiwaku, H., Tanaka, H., Obita, T., Ohuchi, S., Yoshioka, Y., Jin, X., Kondo, K., Fujita, K., Homma, H., et al. (2021). Tau activates microglia via the PQBP1-cGAS-STING pathway to promote brain inflammation. Nat. Commun. *12*, 6565. https://doi.org/10.1038/s41467-021-26851-2.

69. Hupp, S., Förtsch, C., Graber, F., Mitchell, T.J., and Iliev, A.I. (2022). Pneumolysin boosts the neuroinflammatory response to Streptococcus pneumoniae through enhanced endocytosis. Nat. Commun. *13*, 5032. https://doi.org/10.1038/s41467-022-32624-2.

70. Guo, J., Wang, F., Hu, Y., Luo, Y., Wei, Y., Xu, K., Zhang, H., Liu, H., Bo, L., Lv, S., et al. (2023). Exosome-based bone-targeting drug delivery alleviates impaired osteoblastic bone formation and bone loss in inflammatory bowel diseases. Cell Rep. Med. *4*, 100881. https://doi.org/10.1016/j.xcrm.2022.100881.

71. Chin, C., Ravichandran, R., Sanborn, K., Fleming, T., Wheatcroft, S.B., Kearney, M.T., Tokman, S., Walia, R., Smith, M.A., Flint, D.J., et al. (2023). Loss of IGFBP2 mediates alveolar type 2 cell senescence and promotes lung fibrosis. Cell Rep. Med. *4*, 100945. https://doi.org/10.1016/j.xcrm.2023.100945.

72. Singh, A., D'Amico, D., Andreux, P.A., Fouassier, A.M., Blanco-Bose, W., Evans, M., Aebischer, P., Auwerx, J., and Rinsch, C. (2022). Urolithin A improves muscle strength, exercise performance, and biomarkers of mitochondrial health in a randomized trial in middle-aged adults. Cell Rep. Med. *3*, 100633. https://doi.org/10.1016/j.xcrm.2022.100633.

73. Wang, X., Yu, J., Liu, X., Luo, D., Li, Y., Song, L., Jiang, X., Yin, X., Wang, Y., Chai, L., et al. (2022). PSMG2-controlled proteasome-autophagy balance mediates the tolerance for MEK-targeted therapy in triple-negative breast cancer. Cell Rep. Med. *3*, 100741. https://doi.org/10.1016/j.xcrm.2022.100741.

74. Luo, Z., Hu, X., Wu, C., Chan, J., Liu, Z., Guo, C., Zhu, R., Zhang, L., Zhang, Y., Jin, S., and He, S. (2023). Plasma exosomes generated by ischaemic preconditioning are cardioprotective in a rat heart failure model. Br. J. Anaesth. *130*, 29–38. https://doi.org/10.1016/j.bja.2022.08.040.

75. Wang, Y., Guan, X., Gao, C.-L., Ruan, W., Zhao, S., Kai, G., Li, F., and Pang, T. (2021). Medioresinol as a novel PGC-1α activator prevents pyroptosis of endothelial cells in ischemic stroke through PPARα-GOT1 axis. Pharmacol. Res. *169*, 105640. https://doi.org/10.1016/j.phrs.2021.105640.

76. Gao, C., Xu, Y., Liang, Z., Wang, Y., Shang, Q., Zhang, S., Wang, C., Ni, M., Wu, D., Huang, Z., and Pang, T. (2021). A novel PGAM5 inhibitor LFHP-1c protects blood-brain barrier integrity in ischemic stroke. Acta Pharm. Sin. B *11*, 1867–1884. https://doi.org/10.1016/j.apsb.2021.01.008.

77. Wlodarczyk, A., Holtman, I.R., Krueger, M., Yogev, N., Bruttger, J., Khorooshi, R., Benmamar-Badel, A., de Boer-Bergsma, J.J., Martin, N.A., Karram, K., et al. (2017). A novel microglial subset plays a key role in myelinogenesis in developing brain. EMBO J. *36*, 3292–3308. https://doi.org/10.15252/embj.201696056.

78. Kana, V., Desland, F.A., Casanova-Acebes, M., Ayata, P., Badimon, A., Nabel, E., Yamamuro, K., Sneeboer, M., Tan, I.L., Flanigan, M.E., et al. (2019). CSF-1 controls cerebellar microglia and is required for motor function and social interaction. J. Exp. Med. *216*, 2265–2281. https://doi.org/10.1084/jem.20182037.

79. Wan, P., Su, W., Zhang, Y., Li, Z., Deng, C., Li, J., Jiang, N., Huang, S., Long, E., and Zhuo, Y. (2020). LncRNA H19 initiates microglial pyroptosis and neuronal death in retinal ischemia/reperfusion injury. Cell Death Differ. *27*, 176–191. https://doi.org/10.1038/s41418-019-0351-4.

80. Zhang, J., Rong, P., Zhang, L., He, H., Zhou, T., Fan, Y., Mo, L., Zhao, Q., Han, Y., Li, S., et al. (2021). IL4-driven microglia modulate stress resilience through BDNF-dependent neurogenesis. Sci. Adv. *7*, eabb9888. https://doi.org/10.1126/sciadv.abb9888.

81. Al Mamun, A., Chauhan, A., Qi, S., Ngwa, C., Xu, Y., Sharmeen, R., Hazen, A.L., Li, J., Aronowski, J.A., McCullough, L.D., and Liu, F. (2020). Microglial IRF5-IRF4 regulatory axis regulates neuroinflammation after cerebral ischemia and impacts stroke outcomes. Proc. Natl. Acad. Sci. USA *117*, 1742–1752. https://doi.org/10.1073/pnas.1914742117.

82. Lin, R., Zhou, Y., Yan, T., Wang, R., Li, H., Wu, Z., Zhang, X., Zhou, X., Zhao, F., Zhang, L., et al. (2022). Directed evolution of adeno-associated virus for efficient gene delivery to microglia. Nat. Methods *19*, 976–985. https://doi.org/10.1038/s41592-022-01547-7.

83. Chen, J., Jin, J., Zhang, X., Yu, H., Zhu, X., Yu, L., Chen, Y., Liu, P., Dong, X., Cao, X., et al. (2021). Microglial lnc-U90926 facilitates neutrophil infiltration in ischemic stroke via MDH2/CXCL2 axis. Mol. Ther. *29*, 2873–2885. https://doi.org/10.1016/j.ymthe.2021.04.025.

84. Hu, Y., Yao, Y., Qi, H., Yang, J., Zhang, C., Zhang, A., Liu, X., Zhang, C., Gan, G., and Zhu, X. (2023). Microglia sense and suppress epileptic neuronal hyperexcitability. Pharmacol. Res. *195*, 106881. https://doi.org/10.1016/j.phrs.2023.106881.

85. Seo, D.-O., O'Donnell, D., Jain, N., Ulrich, J.D., Herz, J., Li, Y., Lemieux, M., Cheng, J., Hu, H., Serrano, J.R., et al. (2023). ApoE isoform- and microbiota-dependent progression of neurodegeneration in a mouse model of tauopathy. Science *379*, eadd1236. https://doi.org/10.1126/science.add1236.

86. Xu, Y., Johansson, M., and Karlsson, A. (2008). Human UMP-CMP kinase 2, a novel nucleoside monophosphate kinase localized in mitochondria. J. Biol. Chem. *283*, 1563–1571. https://doi.org/10.1074/jbc.M707997200.

87. Renner, M., Flanagan, A., Dejnirattisai, W., Puttikhunt, C., Kasinrerk, W., Supasa, P., Wongwiwat, W., Chawansuntati, K., Duangchinda, T., Cowper, A., et al. (2018). Characterization of a potent and highly unusual minimally enhancing antibody directed against dengue virus. Nat. Immunol. *19*, 1248–1256. https://doi.org/10.1038/s41590-018-0227-7.

STAR★METHODS

KEY RESOURCES TABLE

REAGENT or RESOURCE	SOURCE	IDENTIFIER
Antibodies		
Mouse anti-β-actin	Proteintech	Cat# 20536-1-AP; RRID: AB_10700003
Rabbit anti-Caspase-1	CST	Cat# 89332S; RRID: AB_2923067
Rabbit anti-GSDMD	Abcam	Cat# ab209845; RRID: AB_2783550
Rabbit anti-GSDMD	Abcam	Cat# ab219800; RRID: AB_2888940
Goat anti-IL-1β	R&D Systems	Cat# AB-401-NA; RRID: AB_354347
Rabbit anti-IBA1	Wako	Cat# 01919741; RRID: AB_839504
Goat anti-IBA1	NOVUS	Cat# NB100-1028; RRID: AB_521594
Mouse anti-GFAP	CST	Cat# 3670; RRID:AB_561049
Mouse anti-NeuN	Proteintech	Cat# 66836-1-Ig; RRID: AB_2882179
Rabbit anti-8-OHdG	Bioss	Cat# bs-1278R; RRID: AB_10856120
Rat anti-Ki67	Invitrogen	Cat# 14-5698-82; RRID: AB_10854564
Goat anti-ASC	Abcam	Cat# Ab175449; RRID: AB_3096354
Rat anti-CD11b	Invitrogen	Cat# 14-0112-82; RRID: AB_467108
Rabbit anti-TOMM20	Proteintech	Cat# 11802-1-AP; RRID: AB_2207530
Alexa Flour™ 488 goat anti-rabbit IgG (H + L)	Invitrogen	Cat# A11008; RRID: AB_143165
Alexa Flour™ 633® goat anti-mouse IgG (H + L)	Invitrogen	Cat# A21050; RRID: AB_2535718
FITC–conjugated donkey Anti-rabbit IgG(H + L)	Proteintech	Cat# SA00003-8; RRID: AB_2890899
Cy3 donkey anti-goat IgG (H + L)	Servicebio	Cat# GB21404; RRID: AB_2868507
Cy3 goat anti-rat IgG (H + L)	Servicebio	Cat# GB21302; RRID: AB_2936331
Chemicals, peptides, and recombinant proteins		
NDGA	Sigma	74540
LPS	Sigma	I4524
ATP	Sigma	A8937
Poly-L-lysine	Sigma	P2636
Tamoxifen	Sigma	T5648
DMEM	Invitrogen	11965092
glucose-free DMEM	Invitrogen	11966025
DMEM/F-12	Invitrogen	11330032
MitoSOX	Yeasen	40778ES50
MCSF	Novoprotein	CB34
Lipofectamine 2000	Invitrogen	11668019
Hoechst 33342	Beyotime	C1025
DMSO	Sigma	D8418
H_2O_2	Sigma	88597
Critical commercial assays		
LDH Cytotoxicity Assay Kit	Beyotime	C0017
FastPure Cell/Tissue DNA Isolation Mini Kit	Vazyme Biotech Co.,Ltd	DC112
BCA protein assay	Beyotime	P0012
Human IL-1 beta ELISA Kit	RD	VAL101
CD11b (Microglia) MicroBead	Miltenyi	130-093-636
ATP assay kits	Beyotime	S0027

(*Continued on next page*)

Continued

REAGENT or RESOURCE	SOURCE	IDENTIFIER
Experimental models: Organisms/strains		
CX_3CR1-Cre^{ERT2}	Shanghai Model Organisms Center	NM-KI-200157
Oligonucleotides		
Primer used, see Table S1	Sangon Biotech	N/A
Software and algorithms		
ImageJ	NIH	N/A
Prism	GraphPad	N/A
IMARIS 9.6.2	Bitplane	N/A

RESOURCE AVAILABILITY

Lead contact

Further information and requests for resources and reagents should be direct to and will be fulfilled by the lead contact, Tao Pang (tpang@cpu.edu.cn).

Materials availability

This study did not generate new unique reagents.

Data and code availability

- All data reported in this paper will be shared by the lead contact upon request. This paper does not report original code.
- Any additional information required to reanalyze the data reported in this paper is available from the lead contact upon request.

EXPERIMENTAL MODEL AND SUBJECT DETAILS

Human sample collection and processing

This investigation recruited 31 patients with acute ischemic stroke and 21 age-matched healthy subjects from September 2021 to September 2023. This study was approved by the Ethics Committee of the Second Affiliated Hospital of Nanjing Medical University with written informed consent from ischemic stroke patients or age-matched healthy subjects (Ethics approval number: 2019-KY116). The investigation was accomplished according to the guidelines of the Helsinki Declaration. Firstly, the patients were confirmed with symptoms of acute ischemic stroke based on clinical manifestations and then [66] diagnosed using magnetic resonance imaging (MRI) with diffusion-weighted imaging (DWI). Then, the blood samples from all patients were collected before any therapeutic medication. Approximately 4–5 mL of peripheral blood samples were obtained in EDTA-K_2 anticoagulant tubes, lysed in TRIzol regents, and then stored in a −80°C refrigerator. Ischemic stroke patients and healthy control subjects with the following characteristics were excluded from this study: (1) having other intracranial diseases; (2) having an autoimmune disorder, acute or chronic infectious diseases, hematologic disorders, or a history of surgical surgery in the past year; (3) taking hormones or immunosuppressants within the past 6 months. As previously reported,[66,67] peripheral blood mononuclear cells (PBMC) were sorted using the PBMC isolation kit (Famacs, Nanjing, China) in line with the manufacturer's instructions, the *purity* of *which was* above *90%* for monocytes as determined by flow cytometry. The patient parameters including age, gender, comorbidity, stroke location, collection of blood after stroke (hours/days) were listed in Table S2.

Animals

$CX_3CR1^{Cre/ERT2}$ mice were obtained from the Shanghai Nanfang Research Center for Model Organisms. Wide-type (WT) C57BL/6J mice were obtained from the *Slake Company* (Shanghai, China). All the animal procedures were approved by Animal Ethics Committee of China Pharmaceutical University (No. 2021-01-020) and carried out in accordance with the requirements of the National Institutes of Health for the care and use of experimental animals.

Isolation of primary mouse cortical neurons, astrocytes and microglia

Primary mouse cortical neurons, astrocytes, and microglia were isolated according to previous literature.[8,68] Primary mouse cortical neurons were isolated from *pregnant mice* at embryonic *day* (E) 15-E16.[68] In brief, the brain cortices tissue of fetal mice was removed and placed in Hanks balanced salt *solution (HBSS*). Then, the brain tissue was minced into 2 mm-wide pieces and subsequently immersed in 2 mg/mL papain solution at 37°C for 30 min. After digestion, the dissociated neurons were cultivated in Neurobasal medium supplemented with 2% *B27* and 1% $Gluta^{MAX}$ in an incubator at 37°C with 5% CO_2 until the cells grew mature at 7–9 days. Microglia and astrocytes were obtained from the *mixed glial* population with different attachment methods.[69] Briefly, the *neonatal*

mice (postnatal day *1-2*) were *disinfected with 75%* alcohol, and then the cerebral cortex tissue was carefully removed. After gently dissecting the attached *meninges and* blood *vessels, the minced cerebral tissue pieces were immersed in 0.25% trypsin solution* at 37°C for 6–10 min *before terminating digestion with* 6 mL *DMEM-F12* medium supplemented with 10% FBS. Afterward, the dissociated *mixed glial* population was cultivated in *DMEM-F12* supplemented with 10% FBS. When *mixed glial cells* were grown *to 90–100%* cell *density at 10 days,* the microglia were harvested from the *T75* culture flask after shaking at *180× rpm* for 2 *h. Next, the astrocytes adherent to the T75* culture flask *were digested with 0.25% trypsin solution and cultured in* 12-well *plates (Jet Biofil, Guangzhou)* for *the subsequent experiments*.

METHOD DETAILS

Quantitative real-time PCR (qRT-PCR)

The total RNA was extracted with TRIzol reagents (Vazyme Biotech Co., Ltd, China). Then, one microgram of mRNA was reverse-transcribed into cDNA according to the instruction of cDNA Synthesis Kit (Vazyme Biotech Co., Ltd, China). Subsequently, the first strand cDNA was then applied as a template for PCR amplification with *gene-specific primers* using SYBR Green reagent (Vazyme Biotech Co., Ltd, China) on ABI StepOnePlus sequence detection system. The final gene expression was normalized to 18S *r*RNA. The primers applied in the study are displayed in Table S1.

Western blotting analysis

The Western blotting analysis was conducted as we previously described.[70–74] First, the total protein was extracted using RIRA buffer and then the protein concentrations were determined using the BCA kit (Thermo). After mixing with Laemmli sample buffer, the protein samples were separated electrophoretically and then wet-transferred onto 0.22 μm PVDF membranes (Millipore). After blocking with 5% non-fat dry milk in the Tris-buffered saline (TBS) (pH 7.4) containing 0.1% Tween 20 at room temperature for 2 h, the protein membranes were sequentially immersed with the primary antibody at 4°C overnight and secondary antibody at room temperature for 1 h. Finally, the membranes were quantified using Quantity One gel image analysis system with enhanced chemiluminescence detection reagents. All unprocessed Western blotting images were displayed in Figures S7 and S8.

CMPK2 protein and antibody production

Full length of CMPK2 cDNA was amplified and cloned into the Nco I and Hind III sites on a pET-28a(+) vector with 6×His tag. Subcequently, the recombinant plasmids were transformed into BL21(DE3) bateria and the expression of CMPK2 protein was induced by addition of 0.5 mmol/L IPTG. Then, CMPK2 protein purification was carried out with Ni-IDA-Sepharose CL-6B affinity chromatography column (Sangon Biotech, Shanghai). To prepare CMPK2 antibody, aa 135–265 of CMPK2 was amplified and cloned into pET-28a-SUMO vector. After expression and purification, CMPK2 aa135-265 (1.5 mg/mL) was injected into rabbits, following by screening with ELISA and immunoblots. Lastly, the antisera were collected and affinity-purified for further experiments.

Establishment of focal cerebral ischemia/reperfusion model

The mouse tMCAO model is a well-established model to form focal cerebral ischemia, according to previous literature.[66,75] In short, mice are anesthetized in an animal anesthesia chamber containing 3% isoflurane and then maintained under anesthesia at 2% isoflurane. During the surgery, the mouse body temperature was held at 37 ± 0.5°C with the heating pad. First, after bluntly separating the neck muscle, the common carotid artery (CCA), external carotid artery (ECA), and internal carotid artery (ICA) of the mouse were gently isolated without excessive wounding. Then, the silicone-coated monofilament (1800A, Jialing Biotechnology, China) was introduced from ECA and extended to the anterior cerebral artery to block the opening of MCA. Afterward, the arterial blood flow was occluded to maintain the cerebral ischemia for about 1 h, and the silicone-coated monofilament was subsequently extracted to restore cerebral blood flow. During the surgery, laser speckle flow imaging was used to monitor cerebral cortical blood flow. When cerebral blood flow was dropped below 70%, as assessed by Laser Speckle Imaging analysis system (RWD Biotechnology, China), the tMCAO model was considered to be successfully established. As for the Sham group, the mice were exposed to the same operation without inserting silicone-coated monofilament for 1 h.

To explore the effects of NDGA in short-term neurological deficits in the mouse ischemic stroke model, a total of 60 mice were randomly divided into four groups: sham group, tMCAO plus vehicle group, tMCAO plus NDGA (5 mg/kg or 20 mg/kg) group at 3 h, 6 h, 24 h, and 48 h. In the mice subjected to tMCAO model, 10 mice were excluded from the analysis for unsuccessful operation ($n = 1$) or hemorrhagic transformation ($n = 3$), and 6 mice died intraoperatively ($n = 2$) or postoperatively ($n = 4$). To explore the effects of NDGA and CMPK2 knockdown in short-term neurological deficits in the mouse ischemic stroke model, a total of 148 $CX_3CR1^{Cre/ERT2}$ mice were randomly divided into six groups: sham plus AAV-shCon, sham plus AAV-shCMPK2, tMCAO plus AAV-shCon, tMCAO plus AAV-shCMPK2, tMCAO plus AAV-shCon plus NDGA (20 mg/kg), tMCAO plus AAV-shCMPK2 plus NDGA (20 mg/kg). In the $CX_3CR1^{Cre/ERT2}$ mice subjected to tMCAO model, 24 mice were excluded from the analysis for unsuccessful operation ($n = 3$) or hemorrhagic transformation ($n = 6$), and 15 mice died intraoperatively ($n = 3$) or postoperatively ($n = 12$). To explore the effects of NDGA in long-term neurological deficits in the mouse ischemic stroke model, a total of 84 mice were randomly divided into three groups: sham group, tMCAO plus vehicle group, tMCAO plus NDGA (20 mg/kg) group at 3 h, 6 h, 1 day, 2 days, 3 days, 4 days, 5 days, 6 days, and

7 days. In the mice subjected to tMCAO model, 15 mice were excluded from the analysis for unsuccessful operation (n = 3), or hemorrhagic transformation (n = 3), and 9 mice died intraoperatively (n = 2) or postoperatively overnight (n = 7).

Assessment of cerebral infarct volume and neurological function

2, 3, 5-triphenyltetrazolium chloride (TTC, TCI, Japan) staining was applied to measure cerebral infarct volume. In brief, the mice were sacrificed under deep isoflurane anesthesia. Then, brains were gently dissociated and cut into five coronal brain slices (1–2 mm thick) and subsequently incubated with 2% TTC solution at 37°C for 10 min. Finally, the coronal brain slices were photographed using camera, and the infarct volumes were determined with ImageJ software. The cerebral infarct volume (with correction for brain oedema) (%) was evaluated as follows: (the contralateral hemisphere minus the non-infarct area of the ipsilateral hemisphere)/(the contralateral hemisphere × 2) × 100%.

In this study, Longa's test was used to determine short-term neurological deficits in the mouse ischemic stroke model.[66,75] Moreover, long-term neurological performances were evaluated in mice of each group by the modified neurological severity score (mNSS), foot-fault test, wire-hanging test, and rotarod test at 1, 3, 5, 7, 14, 21 and 28 days after tMCAO as previously demonstrated.[66,75] All the behavioral tests were conducted *in a double-blind* manner.

Immunofluorescence staining

The immunofluorescence staining was conducted as we previously described.[76] Briefly, the dissociated brains were fixed in 4% paraformaldehyde solution for 24 h and then sequentially dehydrated in 15% and 30% sucrose solutions at 4°C for 2–3 days until sunk. Next, the frozen mouse brain tissue was sliced into 16 μm or 40 μm coronal slices using the Leica cryostat microtome. As for immunofluorescence staining, the frozen mouse coronal slices and cells were fixed with 4% formaldehyde and then washed 3 times with phosphate-buffered saline (PBS) (pH 7.4) solution for 5 min. Afterward, the slices were immersed in PBS solution with 10% normal goat serum or donkey serum for 1 h at room temperature to avoid non-specific staining. Next, the slices were sequentially incubated with the primary antibodies at 4°C overnight and secondary antibodies at room temperature for 1 h. And the cell nuclei were counterstained with Hoechst 33342. Finally, the immunofluorescence imaging was acquired and visualized using FV3000 microscope (Olympus, Japan). As for immunofluorescence staining in PBMCs, the experiments were performed at about 1–2 h after blood collection.

Adult mouse microglial isolation and flow cytometry examination

Mouse microglia from adult mouse brains were isolated using the CD11b (Microglia) MicroBeads Kit (Miltenyi Biotec) following the manufacturer's instructions.[77,78] Then, the isolated microglia were blocked with rat anti-mouse CD16/32 for 20 min to avoid non-specific staining. Afterward, the cells were sequentially incubated with FVS780 and fluorochrome-conjugated primary antibodies against $CD11b^+$ or $CD45^+$ in the dark. Finally, the samples were examined with the CytoFLEX flow cytometer (Beckman, USA).

Oxygen-glucose deprivation (OGD) treatment

To mimic the ischemic state for microglia, astrocytes, and neurons, the OGD model was established *in vitro* as previously reported.[8,79] Briefly, the primary mouse microglia, astrocytes, or cortical neurons were replaced with DMEM medium without glucose and FBS (Gibco, USA) in the hypoxia chamber (Billups-Rothenberg Inc, USA) for the indicated time at 37°C with 95% N_2 and 5% CO_2 for the following experiments.

Stereotaxic surgery

For stereotaxic surgery, the head of mouse was placed in the stereotactic frame (RWD Life Science, Shenzhen, China) in a prone position under 2% isoflurane. Then, 1 μL of rAAV-CMV-DIO-mCherry-Loxp-shRNA (Scramble)-WPRE-polyA (5×10^{12} viral genomes/μL) viruses or rAAV-CMV-DIO-mCherry-Loxp-shRNA (CMPK2)-WPRE-polyA (5×10^{12} viral genomes/μL) viruses using AAV-MG1.2 vectors were injected into the target site (0.5 mm anterior to the bregma, 2.0 mm lateral (right) to the sagittal suture, and 1.0 mm from the surface of the skull) of $CX_3CR1^{Cre/ERT2}$ at a rate of 0.05 μL/min with a 30-gauge needle for 20 min using a microsyringe pump (RWD Life Science, Shenzhen, China).[31,80–82] After injecting the *Cre*-dependent virus, the microsyringe remained in position for 10 min before being removed. Subsequently, the mice were held on the heating pad to recuperate from the anesthesia. After 14 days post stereotaxic surgery, the $CX_3CR1^{Cre/ERT2}$ mice were injected intraperitoneally with 75 mg/kg tamoxifen (Sigma, USA) per day for consecutive 5 days to induce *Cre* recombinase expression.[31,80] The AAV transfection area accounted for approximately 19.25 ± 3.26% of the total infarct area and 43.68 ± 5.13% of the cerebral cortex infarct area.[83,84]

In vivo mouse brain magnetic resonance imaging (MRI) scanning

To assess the degree of ischemic stroke in the mice, MRI scanning was conducted at day 14 with the Bruker BioSpec 7.0-T/20-cm MRI scanner (Bruker, Germany).[66,75] First, the mice were anesthetized and placed on the experimental bench in a prone position, with the head fixed at the center of radiofrequency (RF) body transmit coil. Then, the MRI images were obtained using the T2 Star sequence setting: (repetition time (TR) = 3000 ms, echo time (TE) = 45 ms, slice thickness of 0.50 mm, flip angle (FA) = 135°, 20 mm × 20 mm in-plane resolution, and 512 × 256 matrix). The cerebral infarct volume (with correction for brain oedema) (%) was evaluated as follows: (the contralateral hemisphere minus the non-infarct area of the ipsilateral hemisphere)/(the contralateral hemisphere × 2) × 100%.

Three-dimensional (3D) reconstruction

The 40 μm brain slices were sequentially incubated with anti-Iba1 primary antibody at 4°C overnight and Alexa Fluor 488-conjugated secondary antibody at room temperature for 1 h. After staining the cell nuclei with Hoechst 33342, 1024 × 1024-pixel resolution images were captured using FV3000 with 1.0 μm steps in the Z-direction, followed by 3D reconstructions with IMARIS 9.0 software (Bitplane).[31,85] Finally, the process lengths and total branch points were semi-automatically quantified using Imaris software.

LPS-primed NLRP3 inflammasome model in primary mouse microglia cells and human primary monocytes

As previously described, priming the cells with LPS followed by ATP stimulation is an established model to induce the NLRP3 inflammasome activation.[41–43] After seeding on 24-well plates overnight, primary mouse microglia and human primary monocytes were simultaneously treated with ultrapure LPS (100 ng/mL) for 6 h and NDGA at the indicated concentrations, and then stimulated with ATP (3 mM) for 30 min. Eventually, cell lysates and supernatants were collected for further experiments.

Cell transfection

To investigate the effects of target CMPK2 or 5-LOX in cells, primary mouse microglia were transfected with *Cmpk2* siRNA (si-*Cmpk2*), *5-Lox* siRNA (si-*5-Lox*) or negative siRNA using Lipofectamine 2000 reagent (Invitrogen, USA) for 48 h following the guidelines of manufacturer. The sequences of si-*Cmpk2*: GGCUUCUGAAAUAGCUAAATT; si-*5-Lox*: CCCGAGAUAUCCAGUUUGATT.

Analysis of lactate dehydrogenase (LDH) release

The contents of LDH in cell culture supernatant after priming with LPS followed by ATP stimulation or OGD treatment were determined using *LDH* kit (Beyotime Biotechnology, China) under the manufacturer's guidelines. All samples and standards were assessed in triplicate.

Edu staining experiment

To detect newly synthesized mtDNA, EdU detection was conducted using Click-iT EdU Cell Proliferation Kit with Alexa Fluor 488 (Beyotime, China) according to the previous reports.[25] Finally, immunofluorescence imaging was acquired and visualized using FV3000 microscope.

Measurement of total mtDNA

After washing the microglia twice with sterile PBS solution, the microglia were collected to extract the total mtDNA using the FastPure Cell DNA Isolation Mini Kit (Vazyme Biotech Co.,Ltd, China) following the manufacturers' advisement. Then, the mtDNA contents were assessed by qPCR amplification with gene-specific primers.[25] The final mtDNA expression was normalized to nuclear DNA encoding *Tert*. The gene-specific primers for the mtDNA applied in the study are displayed in Table S1.

Enzyme-linked immunosorbent assay (ELISA) for IL-1β cytokine

The concentrations of IL-1β cytokine in cell culture supernatant were determined using the human or mouse IL-1β ELISA kit (RD, USA) in accordance with the manufacturer's guidelines. All samples and standards were assessed in triplicate.

In vitro CMPK2 kinase assay and compounds screening

The CMPK2 kinase assay was performed with 3180 compounds. The compound libraries were obtained from Selleck (L1300, L3800, L8000) and all compounds were dissolved in DMSO at the equivalent concentration. Inhibition of CMPK2 kinase activity was determined using an ADP-Glo Kinase Assay Kit (Promega, USA).[86] Briefly, recombinant human CMPK2 kinase (2 μg/reaction) was mixed with the test compounds in the kinase assay buffer (5 mM $MgCl_2$, 25 mM HEPES pH 7.2, 50 mM Tris-HCl pH 7.6–8.0, 5 μM ATP, 100 μM CMP). To explore the effects of NDGA on CMPK2 enzymatic activity, different concentrations of NDGA were incubated with the CMPK2 kinase in the kinase assay buffer. Lastly, the kinase detection regent was added to determine the luminescence under the Paradigm detection platform (Beckman).

Surface plasmon resonance (SPR) assay

In order to investigate whether NDGA binds with CMPK2 protein directly, the SPR binding experiment was carried out using a Biacore 8K instrument (GE Healthcare).[76,86,87] Recombinant CMPK2 kinase (50 μg) was immobilized on the CM5 chip, followed by injection of NDGA at different concentrations at a flow rate of 30 μL/min for 350 s. Finally, the binding curves and affinity data were recorded and assessed using Biacore Insight evaluation software.

QUANTIFICATION AND STATISTICAL ANALYSIS

Data are displayed as mean ± SD and analyzed by using the software GraphPad Prism 7.0. Depending on the dataset, statistical analysis was carried out using unpaired Student's t test, non-parametric Mann-Whitney test, log rank (Mantel-Cox) test, One-way ANOVA with Bonferroni's corrections, or two-way ANOVA with Bonferroni's corrections with or without repeated measurements, respectively. Differences are recognized statistically significant at $p < 0.05$.